Murachi, T. (1983) in *Calcium and Cell Function* (Cheung, W. Y., Ed.) Vol. IV, pp 377–410, Academic, New York.
Ohno, S., Emori, Y., Imajoh, S., Kawasaki, H., Kisaragi, M., & Suzuki, K. (1984) *Nature (London) 312*, 566–570.
Ohno, S., Emori, Y., Sugihara, H., Imajoh, S., & Suzuki, K. (1987) *Methods Enzymol. 139*, 363–379.
Pontremoli, S., Melloni, E., Michetti, M., Sparatore, B., Salamino, F., Sacco, O., & Horecker, B. L. (1987) *Proc. Natl. Acad. Sci. U.S.A. 84*, 398–401.
Sasaki, T., Yoshimura, N., Kikuchi, T., Hatanaka, M., Kitahara, A., Sakihama, T., & Murachi, T. (1983) *J. Biochem. (Tokyo) 94*, 2055–2061.
Suzuki, K., Ishiura, S., Tsuji, S., Katamoto, T., Sugita, H., & Imahori, K. (1979) *FEBS Lett. 104*, 355–358.
Suzuki, K., Ohno, S., Imajoh, S., Emori, Y., & Kawasaki, H. (1985) *Biomed. Res. 6*, 323–327.
Suzuki, K., Imajoh, S., Emori, S., Kawasaki, H., Minami, Y., & Ohno, S. (1987) *FEBS Lett. 220*, 271–277.
Tapley, P. M., & Murray, A. W. (1985) *Eur. J. Biochem. 151*, 419–423.
Yumoto, N., Kikuchi, T., Sasaki, T., & Murachi, T. (1984) *J. Biochem. (Tokyo) 96*, 1531–1537.
Zeman, R. J., Kameyama, T., Matsumoto, K., Bernstein, P., & Etlinger, J. D. (1985) *J. Biol. Chem. 260*, 13619–13624.

Interaction of Chloroquine with Linear and Supercoiled DNAs. Effect on the Torsional Dynamics, Rigidity, and Twist Energy Parameter†

Pengguang Wu, Lu Song, James B. Clendenning, Bryant S. Fujimoto, A. S. Benight, and J. Michael Schurr*
Department of Chemistry, BG-10, University of Washington, Seattle, Washington 98195
Received March 25, 1988; Revised Manuscript Received June 3, 1988

ABSTRACT: The magnitude and uniformity of the torsion elastic constant (α) of linear pBR322 DNA and supercoiled pBR322 DNAs with high-twist ($\sigma = -0.083$) and normal-twist ($\sigma = -0.48$) are measured in 0.1 M NaCl as a function of added chloroquine/base-pair ratio (chl/bp) by studying the fluorescence polarization anisotropy (FPA) of intercalated ethidium dye. The time-resolved FPA is measured by using a picosecond dye laser for excitation and time-correlated single-photon counting detection. A general theory is developed for the binding of ligands that unwind superhelical DNAs, and the simultaneous binding of two different intercalators is treated in detail. The equilibrium constant (K) for binding chloroquine to linear pBR322 DNA and the number (r) of bound chloroquines per base pair are determined from the relative amplitude ratio of the slow (normally intercalated) and fast (free) components in the decay of the (probe) ethidium fluorescence intensity as a function of chl/bp. For chloroquine binding to supercoiled pBR322 DNAs, the intrinsic binding constant is assumed to be the same as for the linear DNA, but the twist energy parameter E_T (N times the free energy to change the linking number from 0 to 1 in units of k_BT) is regarded as adjustable. Using the best-fit E_T, the binding ratios r are calculated for each chl/bp ratio. Twist energy parameters are also determined for ethidium binding to these supercoiled DNAs by competitive dialysis. For chloroquine binding, we obtain $E_T = 360$ and 460 respectively for the normal-twist and high-twist supercoiled DNAs. For ethidium binding the corresponding values are $E_T = 280 \pm 70$ and 347 ± 50. Like other dye-binding values, these are substantially lower than those obtained by ligation methods. In the absence of chloroquine, the torsion constants of all three DNAs are virtually identical, $\alpha = (5.0 \pm 0.4) \times 10^{-12}$ dyn·cm. For linear pBR322 DNA, the magnitude and uniformity of α remain unaltered by intercalated chloroquine up to $r = 0.19$. This finding argues that the FPA is not significantly relaxed by diffusion of any kinks or solitons. If α_d denotes the torsion constant between a dye and a base pair and α_0 that between two base pairs, then our data imply that α_d/α_0 lies in the range 0.65–1.64, with a most probable value of 1.0. For the supercoiled DNAs, α remains uniform, but its magnitude decreases significantly with increasing intercalated chloroquine through the point where the effective superhelix density vanishes and even up to substantial positive superhelix densities. The significant difference in observed FPA dynamics between the relaxed (by intercalator) supercoiled DNAs and the linear DNA with the same amount of bound chloroquine profoundly contradicts any notion that the local structures and dynamics of such species are equivalent. At very high chl/bp ratios both linear and supercoiled DNAs exhibit evidence of substantial structural changes. The torsion constant increases for the linear DNA but drops for the supercoiled DNAs, which are substantially positively twisted ($\sigma \geq 0.06$) at that point.

Time-resolved fluorescence polarization anisotropy (FPA) measurements on intercalated ethidium dye have been employed to study the rotational dynamics of various DNAs from 10^{-10} to 1.5×10^{-7} s (Thomas et al., 1980a; Wilcoxon et al., 1982; Millar et al., 1982; Madge et al., 1983; Ashikawa et al., 1983, 1984; Thomas & Schurr, 1983; Shibata et al., 1984, 1985; Fujimoto et al., 1985). Previous work in this laboratory (Thomas et al., 1980a; Shibata et al., 1985) demonstrated that the FPA from 1 to 120 ns follows closely the theoretical predictions for a filament with uniform torsional rigidity (Barkley & Zimm, 1979; Allison & Schurr, 1979; Schurr, 1984). For linear DNAs, it was also shown that the apparent torsion constant (α) between base pairs is essentially unaffected by temperature (T) from 0 to 70 °C (Thomas & Schurr, 1983; Wilcoxon & Schurr, 1983), GC content from 34 to 100% (Fujimoto et al., 1985), and spermidine binding in 10 mM

† This work was supported in part by Grants DMB-8403118 from the National Science Foundation (linear DNAs) and by Grant R01-GM29338 from the National Institutes of Health (supercoiled DNAs).

0006-2960/88/0427-8128$01.50/0

NaCl up to about 85% neutralization of the phosphate charge (Wilcoxon et al., 1982). Sensitivity of this FPA experiment to nonuniformity of the torsional rigidity was also demonstrated. Raising the pH to 10.2 in the presence of 40 μM spermidine plus 10 mM NaCl causes a marked decrease in the best-fit values of α obtained on the longer (80 and 120 ns) time spans, though not on the shorter (18 and 36 ns) time spans (Wilcoxon et al., 1982). Such behavior is expected for major rigidity weaknesses with an average separation of 300–400 base pairs. These so-called titratable joints had been detected earlier by dynamic light scattering (DLS) (Thomas et al., 1980b; Lin et al., 1981) and attributed to bound ammonium groups, which stabilize local opening of the DNA and premature titration of the imino protons of T or G (Wilcoxon et al., 1984).

The present study of the effect of intercalated chloroquine on the rotational dynamics of intercalated ethidium was undertaken to address the following questions and concerns.

(1) It is conceivable that the torsion constant of the DNA is substantially weaker in the neighborhood of an intercalated dye and that the torsion constants obtained previously contain a systematic error arising from that. Indeed, Sobell et al. (1983) proposed that ethidium intercalates at the sites of so-called β-kink structures and suggested that the torsional rigidity is 10-fold lower than normal at such sites. The magnitude and uniformity of the observed torsion constants of calf thymus and ϕ29 DNAs are nearly independent of the ethidium/base-pair ratio over the range from 1/600 to 1/50 (Millar et al., 1982; J. H. Shibata, unpublished results). This rules out rigidity decreases by as much as 10-fold at the ethidium-binding site. However, smaller decreases of the torsion constant at the intercalation site might have escaped detection. By using chloroquine, it is possible to examine the magnitude and uniformity of the torsion constant at much higher levels of intercalation without encountering depolarization due to excitation transfer between the ethidium probe molecules. Any significant loss of torsional rigidity at the intercalation sites should then be readily apparent.

(2) It is conceivable that diffusion of kinks, or overdamped solitons, along the chain results in an FPA decay with a functional form similar to the $\exp[-at^{1/2}]$ predicted for torsional deformations. The linear diffusion of kinks along an otherwise stationary (i.e., nonrotating, nontwisting, or nonbending) straight chain is found to give rise to such a functional dependence (Skinner & Wolynes, 1980a,b; Skinner, 1983). Different kinked structures have been proposed for DNA (Sobell et al., 1977, 1983; Crick & Klug, 1975). Diffusing solitons in which the DNA is locally deformed into an open state were proposed as part of a mechanism for hydrogen exchange (Teitelbaum et al., 1975a,b; Englander et al., 1980), although that hypothesis was subsequently eschewed in favor of local base-pair opening (Mandal et al., 1979; Englander & Kallenbach, 1983; Preisler et al., 1984). Recent evidence (Benight et al., 1988) indicates that the solvent-accessible exchanging state is most probably not the unstacked open state of optical melting theory, but a much more probable fluctuation. Large differences in the exchange rates and apparent activation energies of AT and GC base pairs in the same DNA are difficult to reconcile with any mechanism in which exchange is induced by a mobile kink or soliton. Whatever the structure of a kink or overdamped soliton might be, its mobility and stability would almost certainly be substantially affected by high levels of intercalation. If kink diffusion contributes significantly to the depolarization process, then the rate of decay of the FPA would in all likelihood be appreciably altered by extensive intercalation.

(3) A comparison of the torsion potential between an intercalated dye and a base pair with that between two base pairs can be made by examining the FPA up to high concentrations of intercalator. We distinguish those rotations due to collective torsional and flexural deformations of the DNA from local angular wobble of the dye in its binding site (Shibata et al., 1985). There is some evidence that the potential governing local angular wobble is comparable for intercalated ethidium and for a base pair. A rapid relaxation of the FPA with a time constant of 100 ps was resolved by using a streak camera (Magde et al., 1983) and tentatively attributed to 7° rms amplitudes of polar and azimuthal liberation of the dye in a harmonic potential well at its binding site (Shibata et al., 1985; Schurr & Fujimoto, 1988). This amplitude of dye wobble accounts for virtually all of the rapid initial depolarization that is not resolved in single-photon counting experiments, which typically have had instrumental widths (at half-maximum) of 500–600 ps. The rms amplitudes of polar and azimuthal base wobble that must be superimposed on the collective torsional and bending deformations to fit the observed NMR relaxation data of Hogan and Jardetzky (1979) for ^{31}P and of Assa-Munt et al. (1984) and Mirau et al. (1985) for imino protons lie in the range 7–10° (Allison et al., 1982; Langowski et al., 1985a) Schurr & Fujimoto, 1988). The rms amplitudes of local wobble inferred from NMR relaxation data are very sensitive to the assumed molecular geometry. If correct, the similarity in rms amplitudes of the bases (and phosphate groups) on one hand and intercalated dye on the other implies similar libration potentials.

(4) The permanent torsional strain in supercoiled DNAs is generally relaxed with increasing levels of intercalator binding (Bauer & Vinograd, 1970; Bauer, 1978). The question arises whether there is a concomitant increase in torsion constant, as would be anticipated for a highly anharmonic torsion potential.

The free-energy of supercoiling has been measured by essentially two different techniques: the ligation method and the dye-binding method. In the ligation method, an equilibrium distribution of topoisomers with different linking-number differences is created by ligating relaxed (nicked) circles. This distribution is determined directly by analysis of the band intensities in gel electrophoresis, and the free-energy difference between the different species is determined from the ratios of their populations by using simple thermodynamics (Pulleyblank et al., 1975; Depew & Wang, 1975; Shore & Baldwin, 1983; Horowitz & Wang, 1984). The results are usually expressed in terms of the twist energy parameter E_T, which is defined as N times the free energy to change the linking-number difference from 0 to 1 (i.e., to introduce one superhelical turn) in units of k_BT, where N is the total number of base-pairs. A theoretical discussion of the connection between the twist energy parameter E_T and the elementary torsion constant α and bending constant κ_β between base pairs is given in Appendix A. Empirically, E_T is found to be independent of N for long DNAs with $N > 2000$ base pairs (Shore & Baldwin, 1983; Horowitz & Wang, 1984). Reported values of the twist energy parameters determined by the *ligation* method for various long DNAs are listed in Table I. These values fall in the range 1000 ± 100, except for two values near 1600. The origins of the two unusually high values, which deviate by much more than the experimental error, are not the focus of the present work.

The dye-binding method is based on the fact that intercalating dyes remove superhelical turns, hence also torsional strain, and this decrease in supercoiling free-energy contributes

Table I: Twist Energy Parameters Determined by the Ligation Method

DNA	[salt] (mM)	E_T	authors
PM2	10	1000	Depew and Wang (1975)
fd	10	920	Depew and Wang (1975)
SV40	10	1110	Depew and Wang (1975)
E. coli 15	10	1560	Depew and Wang (1975)
PM2	200	985	Pulleyblank et al. (1975)
ColE1	200	1115	Pulleyblank et al. (1975)
Minicol	200	1065	Pulleyblank et al. (1975)
pBR322	60	1130	Horowitz and Wang (1984)
pBR322	60	1610	Shore and Baldwin (1983)

Table II: Twist Energy Parameters Determined by the Dye-Binding Method

DNA	$-\sigma$	salt	E_T	authors
		Ethidium		
PM2	0.110	3 M CsCl	537	Hsieh and Wang (1975)
λb2b5c	0.051	3 M CsCl	527	Hsieh and Wang (1975)
SV40	0.065	5.8 M CsCl	495	Bauer and Vinograd (1970)
λ	0.072	0.1 M NaCl	1246[a]	Hinton and Bode (1975)
λ	0.078	0.4 M NaCl	533[a]	Hinton and Bode (1975)
λ	0.090	1.0 M NaCl	507[a]	Hinton and Bode (1975)
pBR322	0.048 ± 0.005	0.1 M NaCl	280 ± 70	this work
pBR322	0.083 ± 0.007	0.1 M NaCl	347 ± 50	this work
		Chloroquine		
pBR322	0.048 ± 0.005	0.1 M NaCl	360	this work
pBR322	0.083 ± 0.007	0.1 M NaCl	460	this work

[a] Calculated from published data of Hinton and Bode (1975) by using eq 4.

to enhance binding of the dye. In this method, the twist energy parameter is determined from the decrease in effective binding constant as progressively more dye is bound (Bauer & Vinograd, 1970; Hsieh & Wang, 1975). A theoretical discussion of the effect of binding one and two different intercalating dyes on the supercoiling free energy is presented in Appendix A. The corresponding binding isotherms are derived and expressed in terms of the twist energy parameter in Appendix B. Literature values measured by the *dye-binding* technique are listed in the top part of Table II. With but one exception, these values fall in the range $E_T = 500 \pm 50$, which is only half the values determined by the ligation technique. Depew and Wang (1975) state that they obtained a value $E_T = 1200$ for supercoiled PM2 DNA from the ethidium-binding method "in the ligase reaction medium", which contains 50 μg/mL BSA and excess Mg^{2+} in addition to 10 mM Tris buffer.

A prime question is why the dye-binding method usually gives values that are only half the values provided by the ligation method. Certaintly, the dye-binding method requires additional assumptions. One critical assumption is that the dye does not alter the twisting and bending rigidity of the filament at the site of binding or elsewhere. It is also assumed that extensive dye binding induces no change in intrinsic binding constant, no change in unwinding angle, no change in the type of secondary structure apart from local unwinding, so the energetics is governed by simple deformation, and no change in tertiary structure (e.g., from interwound to toroidal). Most of the previous dye-binding measurements were carried out by using ethidium, which conceivably could exhibit singular behavior of some kind. Finally, we note that all of the high values, $E_T \geq 1000$, in Tables I and II are measured at fairly low salt (≤0.2 M), whereas the low values, $E_T = 500 \pm 50$, are all measured at fairly high salt (≥0.4 M). This suggests the possibility that a salt-induced change in secondary and/or tertiary structure might account for the observed differences.

The present studies of ethidium and chloroquine binding to supercoiled pBR322 DNA and of the effect of chloroquine on the torsional rigidity (as probed by ethidium) were undertaken to address the following concerns.

(1) Any change in torsional rigidity at the dye-binding site, or elsewhere, would violate a critical assumption in the analysis of the dye-binding data and invalidate the twise energy parameters obtained therefrom. It is essential to determine whether or not such a change occurs, especially at the comparatively high binding levels usually examined in dye-binding studies.

(2) It is conceivable that the secondary structure and rigidity of *supercoiled* DNA/chloroquine complexes with vanishing superhelix density are not identical with the secondary structure and rigidity of *linear* DNA/chloroquine complexes with the same amount of bound intercalator, contrary to prevailing belief. This cornerstone of the dye-binding analysis has never been tested or even questioned.

(3) It is conceivable that ethidium binding yields anomalously low twist energy parameters, $E_T = 500 \pm 50$, but another intercalating dye might not. To test this possibility we determine the twist energy parameter using chloroquine as well as ethidium.

(4) It is conceivable that low values of the twist energy parameters ($E_T = 500 \pm 50$) are obtained only at salt concentrations greater than 0.4 M but not at salt concentrations less than 0.2 M. To test this possibility, twist energy parameters are determined in 0.1 M NaCl by using both ethidium and chloroquine.

(5) It is conceivable that the twist energy parameter depends in some way on the initial superhelix densities of the samples. To thest this possibility, twist energy parameters are determined for two different samples of pBR322 DNA with different initial superhelix densities.

It should be emphasized that the present FPA studies are all conducted in 0.1 M NaCl at very low levels of bound ethidium (≤1 ethidium/300 base-pairs), which is used merely to probe the effects of chloroquine binding. We investigate the effects of chloroquine binding on three different samples of pBR322 DNA: (1) linearized, (2) supercoiled (normal-twist), and (3) supercoiled (high-twist).

In very low salt (3 mM), the binding of chloroquine and its effect on the torsional rigidity differ somewhat from that reported here. Even in 0.1 M NaCl, other intercalators, such as proflavine, quinacrine, and 9-aminoacridine, have different effects on the torsional rigidity. The effect of ethidium itself on the torsional rigidity is obscured by excitation transfer, which dominates the fluorescence depolarization at high binding levels. Extensive simulations have been performed to separate the contributions of excitation transfer and rotational motions in that case. These other studies will be described in subsequent papers. At that time we shall undertake a comparison of the steady-state FPA results of Genest et al. (1985) for proflavine with our somewhat different findings in regard to its effects on the torsional rigidity.

Materials and Methods

Supercoiled pBR322 DNA (4363 base pairs) was prepared from cells grown in either L-broth or M-9 media according to procedures described earlier (Langowski et al., 1985a,b). The DNA from the cells grown in L-broth exhibited normal superhelix density ($\sigma = -0.048$), whereas the cells grown in

M-9 exhibited a high value ($\sigma = -0.083$). Upon completion of the FPA measurements, less than 10% of the normal-twist ($\sigma = -0.048$) supercoiled DNA was relaxed, but about 20% of the high-twist ($\sigma = -0.083$) supercoiled DNA was relaxed. These DNAs were characterized by gel electrophoresis in 1% agarose containing Tris–borate buffer (90 mM Tris, 90 mM boric acid, 2 mM EDTA). The (absolute) linking-number difference (Δl) of the normal-twist supercoiled DNA was determined in the conventional way by relaxing several samples of this DNA using topoisomerase I (Bethesda Research Co.) in the presence of various amounts of ethidium dye. The linking-number differences for the medium topoisomers of the more relaxed samples (after removing ethidium) could be directly counted off in a gel without chloroquine. The native and various relaxed samples were then run in a gel containing sufficient chloroquine to resolve the topoisomers of the native supercoiled DNA. It was possible to count the number of topoisomer bands from its medium topoisomer up to the relaxed position and back down to the medium topoisomer of a more relaxed sample with known linking-number difference, which was positively supercoiled in that concentration of chloroquine. For the normal-twist sample, the median linking-number difference was $\Delta l = -(20 \pm 2)$, corresponding to a superhelix density $\sigma = -(0.048 \pm 0.005)$. By running the normal-twist and high-twist samples in the same gel containing chloroquine, it was possible to count off the number of topoisomer bands (15 ± 1) separating the medium topoisomers of each sample. Thus, for the high-twist sample $\Delta l = -(35 \pm 3)$ and $\sigma = -(0.083 \pm 0.007)$.

Supercoiled pBR322 DNA was linearized by *Eco*RI and then extensively extracted with buffer phenol, ether extracted, and dialyzed against the standard buffer. On a 1% agarose gel containing Tris–borate buffer, this sample exhibited a single band migrating at the same position as a known linearized pBR322 DNA. Protein contamination was low, as indicated by the absorbance ratio, $A_{260}/A_{280} = 1.96$. The concentrations of linearized, normal-twist supercoiled, and high-twist supercoiled DNA samples were estimated from A_{260} to be 26.7, 48.6, and 19.7 μg/mL, respectively. Ethidium was added to provide a dye/base-pair ratio of about 1/300.

Chloroquine and ethidium were purchased from Sigma Chemical Co. and used without further purification. Chloroquine solutions were prepared by series dilution in distilled water. The concentrations were arranged so that with each addition to the DNA sample (1.1 mL) there was no significant volume change. This was achieved by pipetting 5–8 μL each time. Chloroquine was added to the DNA solutions at least 2–3 days before each measurement to allow time for equilibration. The chloroquine concentration is expressed in terms of added chloroquine per base pair, or simply chl/bp.

The linearized and supercoiled pBR322 DNAs were checked on 1% agarose gels containing Tris–borate buffer (with no chloroquine) after the final additions of chloroquine. They ran at the same position as before the chloroquine titration, which implies that no irreversible structural changes were induced by the chloroquine under these conditions.

FPA measurements were carried out in a standard buffer: 0.1 M NaCl, 10 mM Tris, and 10 mM EDTA. The pH was 8.5 for measurements on the linear and normal-twist supercoiled DNA but was 7.5 in the case of the high-twist supercoiled DNA. The sample cell was thermostated at 20 °C.

FPA measurements were performed by using a picosecond pulsed dye-laser system and electronic apparatus for time-correlated single-photon counting. Details of the instrumentation and data analysis techniques were described previously (Thomas et al., 1980a; Thomas & Schurr, 1983). The excitation wavelength was 575 nm, and the fluorescence emission was collected at 645 nm. Chloroquine exhibits no absorbance at wavelength longer that 500 nm; hence, it is never excited, and there is no possibility of depolarization by excitation transfer between chloroquine and ethidium. As expected, chloroquine–DNA solutions without ethidium exhibit no emission as 645 nm.

Competitive dialysis measurements were carried out in a microdialysis cell purchased from Fisher Scientific Corp. Its two 1-mL chambers were separated by a dialysis membrane with a 6000 molecular weight cutoff. The DNA samples were present in the dialysis buffer: 0.1 M NaCl, 10 mM Tris, and 1 mM EDTA, pH 8.5. For dialysis of linear pBR322 DNA against normal-twist supercoiled pBR322 DNA, the two samples were first dialyzed separately against a large volume of dialysis buffer, and their concentrations were then adjusted to be equal ($A_{260} = 0.81$). Equal volumes of these samples were loaded into the opposing dialysis chambers. An amount of ethidium equivalent to 1 ethidium per 400 *total* base pairs (of linear *and* supercoiled DNA in *both* chambers) was then added to the chamber containing the linear DNA. The sealed microdialysis cell was then wrapped with aluminum foil to shield against UV light and shaken continuously at room temperature ($\cong$20 °C) for at least 4 days.

For the dialysis of normal-twist supercoiled pBR322 DNA vs high-twist supercoiled pBR322 DNA, the volumes and buffers on either side were identical, but the concentrations were slightly different [A_{260}(normal-twist) = 0.81, A_{260}(high-twist) = 0.79]. The final dye distribution between the chambers were scaled accordingly. This experiment was performed at 1 ethidium per 20 *total* base pairs. This ratio is in the typical range of most previous dialysis studies.

At the conclusion of the dialysis, the steady-state fluorescence intensities of the samples in both chambers were measured by using our FPA detection system, as well as a commercial fluorometer (Perkin-Elmer Model 650-10S), and the intensity ratios were used to calculate the pertinent twist energy parameters as described below. Under the conditions of these dialysis experiments, essentially all of the ethidium is bound. In addition, the quantum yield of the free ethidium is only about $^1/_{12}$ that of the intercalated species. In fact, free dye contributes less than 1% of the total fluorescence intensity in any of our samples, which is less than the experimental error. Thus, we can regard all of the intensity as arising from intercalated dye without introducing significant error.

Data Analysis

FPA. The theoretical FPA expression is given by (Schurr, 1984)

$$r(t) = \frac{I_{\parallel}(t) - I_{\perp}(t)}{I_{\parallel}(t) + 2I_{\perp}(t)} = r_0 \sum_{n=0}^{2} I_n C_n(t) F_n(t) \qquad (1)$$

where $I_{\parallel}(t)$ and $I_{\perp}(t)$ are the fluorescence intensities with polarizations parallel and perpendicular, respectively, to that of an infinitesimally short exciting pulse. The I_n are trigonometric factors:

$$I_0 = (\tfrac{3}{2}\cos^2\epsilon - \tfrac{1}{2})^2$$
$$I_1 = 3\cos^2\epsilon \sin^2\epsilon \qquad (2)$$
$$I_2 = \tfrac{3}{4}\sin^4\epsilon$$

where $\epsilon = 70.5°$ is the polar angle between the helix axis and the transition moment of the dye (Schurr & Fujimoto, 1988).

The twisting correlation functions $C_n(t)$ for such a long DNA are assumed to obey the intermediate zone formula (Barkley & Zimm, 1979; Allison & Schurr, 1979)

$$C_n(t) = \exp\left[-\frac{n^2 k_B T}{(\pi\alpha\gamma)^{1/2}} t^{1/2}\right] \quad (3)$$

wherein α is the adjustable torsion constant between base-pairs and γ is the friction factor per base pair for azimuthal rotation of the DNA about its helix axis. We adopt our usual value $\gamma = 6.15 \times 10^{-23}$ dyn·cm·s at $T = 20$ °C, which corresponds to a hydrodynamic cylinder radius of 12 Å in H_2O. This hydrodynamic radius for azimuthal rotation was measured for restriction fragments containing 43 and 69 base pairs (Wu et al., 1987). The tumbling correlation functions are taken to be $F_n(t) = 1.0$. The α values obtained under this assumption are lower bounds to the true values. If one employs instead the expression of Barkley and Zimm (1979) for the tumbling correlation function with a persistence length of 500 Å, the best-fit values of α are increased by a factor of 1.9, but no other conclusions are altered (Shibata et al., 1985).

By use of the measured instrumental profile, the emission data are deconvoluted by a least-squares convolute and compare approach (Thomas et al., 1980a; Thomas & Schurr, 1983). The true sum response to a δ-function exciting pulse is assumed to be

$$S(t) = A_S\delta(t) + S_1(t) + S_2(t)$$

where the δ-function accounts for Raman scattered light from the solvent and $S_1(t)$ and $S_2(t)$ are exponential terms that account for emission from intercalated ($\tau_1 = 21 \pm 1$ ns) and nonintercalated ($\tau_2 = 1.5$–2.5 ns) ethidium. There are three adjustable amplitudes and two adjustable decay times. The true difference response is assumed to be

$$D(t) = r_S A_S\delta(t) + r_1(t)S_1(t) + r_2(t)S_2(t)$$

where r_S is the anisotropy of the scattered light and $r_1(t)$ and $r_2(t)$ are the anisotropy functions for intercalated and nonintercalated dye. Typically, r_S is about 0.3 in our experiments. When $S_1(0)/S_2(0) \geq 15$, then the $r_2(t)S_2(t)$ term can be ignored. That is, the same value of the best-fit torsion constant is obtained from each of the following procedures: (1) use $A_S r_S\delta(t) + r_1(t)S_1(t) + \exp(-t/T_2)S_2(t)$ and set $T_2 = 85 \times 10^{-12}$ s, as measured for free dye by using a Hammamatsu R2809U microchannel plate tube; (2) set $r_2(t) = 0$ and use just $A_S r_S\delta(t) + r_1(t)S_1(t)$; (3) use $A_S r_S\delta(t) + r_1(t)[S_1(t) + S_2(t)]$ but delete the first 4 ns from the fit. However, when $S_1(0)/S_2(0) \leq 10$, as is the case when chloroquine is present at high concentrations, the $r_2(t)S_2(t)$ term is no longer negligible. Moreover, it appears that a significant fraction (roughly 15%) of the nonintercalated dye moves with the DNA rather than as free dye. In view of this complication, we elect to use procedure 3 above. Use of fast Fourier transforms to perform the convolution in the second deconvolution step has decreased the data reduction time by about 5-fold. The adjustable parameters in the anisotropy decay are the initial amplitude r_0 and the torsion constant α.

After the supercoiled pBR322 DNA was linearized, its torsion constant was checked each week for three consecutive weeks. This sample showed no change in the three measurements and is therefore assumed to be in a relatively stable conformation. Some linearized pBR322 DNA samples that we have studied display remarkable evolution of the torsion constant over periods up to 12 weeks, but this sample does not.

Competitive Dialysis. In analyzing the results of competitive dialysis experiments, we use the binding isotherm in eq 4, below, which is a special case of an equation (B29) derived in Appendixes A and B. In the derivation it is assumed that ethidium binding is random and obeys the nearest-neighbor exclusion model without any additional cooperativity. For the comparatively low dye/base-pair ratios ($\leq 1/20$) prevailing in our competitive dialysis experiments, strict validity of these assumptions is not required. However, for the simultaneous binding of chloroquine and ethidium at relatively high levels of total bound intercalator, the validity of these assumptions is an important issue.

For high molecular weight *native* DNA, the binding of ethidium can generally be described by random binding with nearest-neighbor exclusion, but without additional cooperativity (Bauer & Vinograd, 1970; Bresloff & Crothers, 1981; Macgregor et al., 1985; Chandrasekaran et al., 1985; Wilson et al., 1985). Only *Escherichia coli* (chromosomal) DNA from Sigma Chemical Co. and Worthington Biochemicals Co. is reported to show cooperative binding of ethidium (Winkle et al., 1982; Lamos et al., 1986). However, we have also investigated ethidium binding to *E. coli* DNA purchased from both Sigma and Worthington using the same fluorometric assay and experimental conditions employed by Graves and Krugh (1983), including even the same excitation and emission wavelengths and slit widths. We find no evidence of cooperative binding in our samples of *E. coli* DNA.

Neither ethidium (Waring, 1965; Le Pecq & Paoletti, 1967; Müller & Crothers, 1975) nor chloroquine (Cohen & Yielding, 1965) shows a dependence of binding constant on overall base composition. However, different nucleoside monophosphates (Cohen & Yielding, 1965) interact with chloroquine to somewhat different extents.

For binding to oligomers, the results concerning binding-site preference are not clear-cut. While the majority of studies on dinucleotides show some preference for pyrimidine–purine sequences (Krugh et al., 1975; Krugh & Reinhardt, 1975; Reinhardt & Krugh, 1978; Dahl et al., 1982), at least one experiment shows no such preference (Jones et al., 1987). Studies on tetramers also indicate a binding preference for pyrimidine–purine sequence (Patel & Canuel, 1976, 1979; Kastrup et al., 1978). However, studies on heptamers show no preference for pyrimidine–purine over other sites (Nelson & Tinoco, 1984).

Footprinting techniques have been used to study the specific binding sites of intercalators (Van Dyke et al., 1982; Scamrov & Beanealashvilli, 1983; Van Dyke & Dervan, 1984; Hertzberg & Dervan, 1984; Fox & Waring, 1984; Low et al., 1984). Van Dyke et al. (1982) employed the ethidium analogue methidiumpropyl-EDTA–Fe(II) (MPE-Fe) to demonstrate that cutting of plasmid pBR322 DNA was relatively nonspecific. Hertzberg and Dervan (1984) demonstrated that MPE-Fe and ethidium exhibit very similar binding to DNA. From these observations, we infer that ethidium binds in a relatively nonspecific random manner to pBR322 DNA, as assumed in the derivation of eq 4.

The predicted binding isotherm is

$$r/C = K \exp[a(r^* - r)](1 - 2r)^2/(1 - r) \quad (4)$$

The binding ratio r is the number of bound dye molecules per base pair, C is the concentration of free dye, and K is the intrinsic binding constant. The factor $(1 - 2r)^2/(1 - r)$ represents the availability of sites. The binding ratio at which the superhelical turns are completely relaxed is $r^* = -\Delta l \cdot (360)/\phi N$, where Δl is the (usually negative) linking-number difference of the supercoiled DNA (defined in Appendix A), N is the total number of base pairs in the DNA, and ϕ is the unwinding angle for intercalated dye. The exponential

coefficient is given by eq B31 and A20 as $a = 2E_T(\phi/360)^2$, where E_T is the twist energy parameter, which is defined in terms of more elementary quantities in eq A20. An equation of the form of eq 4 holds for the binding of a single intercalating dye to each kind of DNA. It is assumed that the intrinsic binding constant K is the same for all three conformers of pBR322 DNA, namely, the linear, normal-twist supercoiled, and high-twist supercoiled forms. The free dye concentration is assumed to be the same on each side of the microdialysis membrane. Thus, we can take ratios of the isotherms for any two competitively dialyzed species with the result

$$\frac{r_2}{r_1} = \exp[a_2(r_2^* - r_2) - a_1(r_1^* - r_1)]\frac{(1 - 2r_2)^2}{(1 - r_2)}\frac{(1 - r_1)}{(1 - 2r_1)^2} \quad (5)$$

In the dialysis of linear (1) vs normal-twist supercoiled (2) DNA at 1 added ethidium per 400 base pairs, it is found that $r_2/r_1 = 1.2 \pm 0.05$. The amount of ethidium present is so small that $r_2, r_1 \leq 0.0025$. Thus, the ratio of site-availability factors can be set to 1.0. For linear DNA, $a_1 = 0$. Also, for $\Delta l = -(20 \pm 2)$ turns, $r_2^* = 0.063 \pm 0.006$, so $r_2^* \gg r_2$. As will be evident, $a_2 r_2^* < 1.0$, so $a_2 r_2 \ll 1.0$. Hence it is safe to neglect also $a_2 r_2$. With these considerations in mind, the r_2/r_1 datum is analyzed by using $r_2/r_1 = \exp(a_2 r_2^*)$. The result is $a_2 = 2.89 \pm 0.72$, and $E_T = 280 \pm 70$. This value is included in Table II.

In the dialysis of normal-twist supercoiled DNA (1) vs high-twist supercoiled DNA (2) at 1 added ethidium per 20 total base pairs, it is found that $r_2/r_1 = 1.17 \pm 0.002$. The ratio of site availability factors can be estimated by using $r_1 \cong 0.05$ and $r_2 \cong (1.17)(0.0500) = 0.0585$ to be $(0.828)/(0.852) = 0.97$. For $\Delta l = -(35 \pm 3)$ turns, $r_2^* = 0.111 \pm 0.011$. Using $r_1^* = 0.063 \pm 0.006$ (estimated above) for the normal-twist supercoiled DNA, we obtain $r_2^* - r_1^* = 0.048 \pm 0.007$. One can also estimate that $r_2 - r_1 \cong 0.0085$. In this case, a_1 and a_2 should have the same value, so $a_2 r_2 - a_1 r_1 \ll a_2 r_2^* - a_1 r_1^*$. As will be evident, $a_2 r_2^* - a_1 r_1^* < 1.0$, hence $a_2 r_2 - a_1 r_1 \ll 1.0$ and can be neglected. With these considerations in mind, the r_2/r_1 datum is analyzed by using $\exp[a_2 r_2^* - a_1 r_1^*] = (0.97)^{-1}(r_2/r_1)$. From this point, the analysis can follow either of two routes. In the first, we use $\exp[a_1 r_1^*] = 1.2 \pm 0.05$, as measured in the dialysis of linear vs normal-twist supercoiled DNA. The result is $a_2 = 3.33 \pm 0.52$, and $E_T = 320 \pm 50$. In the second procedure, we assume that $a_2 = a_1 = a$. The result is $a_2 = 3.91 \pm 0.67$, and $E_T = 375 \pm 75$. Comparable E_T values are thus obtained from both methods. The average of these two values for the high-twist supercoiled DNA, namely, $E_T = (320 + 375)/2 = 347$, is included in Table II.

Chloroquine Binding Parameters. Except at the very highest added chloroquine per base-pair ratios (chl/bp = 25 and 100), the decay of the ethidium fluorescence intensity of all three DNAs exhibits a large amplitude (A_b) of slow component that is identified with intercalated dye and a small amplitude (A_f) of fast component that is identified with free dye. The *ratios* A_b/A_f of fluorescence decay amplitudes of the intercalated and free ethidium as a function of the *added* chloroquine per base pair (chl/bp) are presented for linear DNA in Figure 1 and for the normal-twist and high-twist supercoiled DNAs in Figure 2. In all three cases, the relative amplitude of the bound ethidium fluorescence falls off at high (chl/bp) ratios, as the chloroquine competes with ethidium for the same binding sites. With appropriate assumptions regarding the binding, we can analyze these *ethidium* fluorescence intensity ratios to obtain the binding parameters for *chloroquine* and determine the *chloroquine* binding ratios

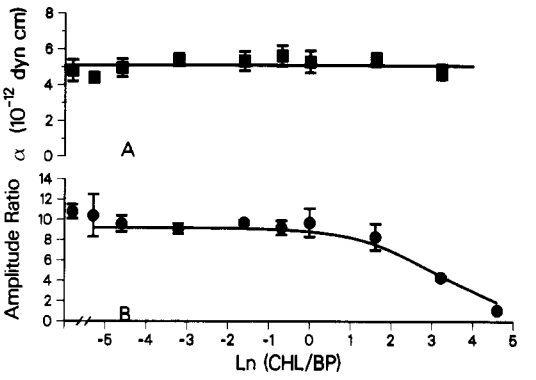

FIGURE 1: Experimental data for linear pBR322 DNA: (A) Torsion constant α (squares) and (B) ratio (A_b/A_f) of the amplitude of the slow (intercalated) and fast (free) components in the decay of the ethidium fluorescence intensity vs added chloroquine per base pair (chl/bp). The DNA is present in 0.1 M NaCl, 10 mM Tris, and 10 mM EDTA, pH 8.5, at 20 °C, and ethidium is present at 1 dye/300 bp. The best-fit theoretical curve (solid line) is calculated from eq 8 and 9 by using the optimum values $K = 381$ M^{-1} and $K_E' = 2.28 \times 10^5$ M^{-1}, as described in the test. The calculated binding ratios (r) corresponding to each experimental value are presented in Table III.

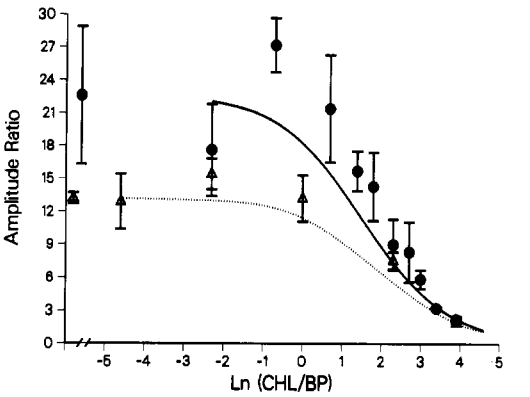

FIGURE 2: Experimental binding data for supercoiled pBR322 DNAs: Ratio (A_b/A_f) of the slow (intercalated) and fast (free) components in the decay of the ethidium fluorescence intensity vs added chloroquine per base pair (chl/bp). Data for normal twist ($\sigma = -0.048 \pm 0.005$) supercoiled DNA are denoted by triangles. Data for high-twist ($\sigma = -0.083 \pm 0.007$) supercoiled DNA are denoted by filled circles. These DNAs are present in 0.1 M NaCl, 10 mM Tris, and 10 mM EDTA, at 20 °C. The pH is 8.5 for the normal-twist form and 7.5 for the high-twist form. The best-fit theoretical curves are calculated from eq 8 and 9, as described in the text. For the normal-twist supercoiled DNA (dotted line), the optimum values are $E_T = 360$ and $K_E' = 1.42 \times 10^5$ M^{-1}. For the high-twist supercoiled DNA (solid line), the optimum values are $E_T = 460$ and $K_E' = 4.45 \times 10^5$ M^{-1}. The calculated binding ratios (r) corresponding to each experimental value of chl/bp are presented in Tables IV and V.

r (number of *bound* dyes per base pair) for each (added) chl/bp ratio.

The fluorescence decay amplitudes are related to the concentrations of free (C_E^f) and intercalated (C_E^b) ethidium by

$$A_b = L\epsilon_b(\lambda_{ex})k_b(\lambda_{em})C_E^b$$

$$A_f = L\epsilon_f(\lambda_{ex})k_f(\lambda_{em})C_E^f$$

where $\epsilon_b(\lambda_{ex})$ and $\epsilon_f(\lambda_{ex})$ are the molar absorbances at the excitation wavelength, λ_{ex}, and $k_b(\lambda_{em})$ and $k_f(\lambda_{em})$ are the emission rates at the emission wavelength, λ_{em}, for bound and free ethidium, respectively. L is an instrumental constant that has the same value for bothy bound and free dye in any given experiment. The fluorescence efficiency ratio, defined by $Q = \epsilon_b(\lambda_{ex})k_b(\lambda_{em})/\epsilon_f(\lambda_{ex})k_f(\lambda_{em})$ varies with both excitation and emission wavelength. From the ratio of steady-state fluorescence intensities of samples containing free dye and

bound dye (1/300 bp) with the same number of ethidium molecules, we measure the efficiency factor $Q = 0.45$ at $\lambda_{ex} = 575$ nm and $\lambda_{em} = 645$ nm for both linear and supercoiled DNAs. The concentration ratio of bound and free ethidium is related to the ratio of fluorescence amplitudes by

$$\frac{A_b}{A_f} = Q\frac{C_E{}^b}{C_E{}^f} \tag{6}$$

In practice, however, there is significant uncertainty in the value of Q, due to uncertainty in λ_{ex}, which may change upon realignment of the laser system due to slack, or backlash, in the monochromator drive. Any given set of experiments on a particular DNA is performed entirely between alignments, so Q should remain constant for such a data set. However, Q may exhibit somewhat different values for data taken before and after a realignment. Thus, equilibrium constants determined by this technique for ethidium binding to the three different forms of pBR322 DNA are *not* sufficiently accurate to determine the twist energy parameters. However, only the constancy of Q for all data on a given DNA is required to determine the intrinsic binding constant K for chloroquine on linear DNA or the twist energy parameter for chloroquine binding to the supercoiled DNAs.

When the bound chloroquine vastly exceeds the bound ethidium, the binding isotherm for chloroquine is given by eq 4, but now r, r^*, K, $a = 2E_T(\phi/360)^2$, and ϕ apply to chloroquine. In excess *chloroquine*, the binding isotherm for *ethidium* is given by

$$\frac{r_E}{C_E} = K_E \exp[a_{EC}(r^* - r)](1 - 2r)^2/(1 - r) \tag{7}$$

wherein r_E and $C_E \equiv C_E{}^f$ apply to ethidium and $a_{EC} = 2E_T\phi\phi_E/(360)^2$, where ϕ_E applies to ethidium. The site availability factor in eq 7 depends only on the *chloroquine* binding ratio r. These results are derived in Appendix B (cf. eq B28, B29). Combining eq 6 and 7 yields

$$\frac{A_b}{A_f} = K_E'C_{bp}{}^0 \exp[a_{EC}(r^* - r)](1 - 2r)^2/(1 - r) \tag{8}$$

where $K_E' = QK_E$ and $C_{bp}{}^0$ is the total concentration of base pairs. Using the definition x = chl/bp and the chloroquine conservation relation, $rC_{bp}{}^0 + C = xC_{bp}{}^0$, eq 4 can be written as

$$\frac{r(1 - r)}{(x - r)(1 - 2r)^2} = KC_{bp}{}^0 \exp[a(r^* - r)] \tag{9}$$

Equations 8 and 9 are used to analyze the A_b/A_f vs r data for each of the three DNAs. However, a and a_{EC} are set to 0 for the linear DNA.

The quantity $C_{bp}{}^0$ is regarded as a precisely known constant for all three measurements on a particular (linear or supercoiled) DNA. The experimental data consist of the corresponding labeled pairs:

$$\{x_1, (A_b/A_f)_1; \ldots; x_N, (A_b/A_f)_N\}$$

The chl/bp ratios x_i are precisely known experimental variables, so the experimental error resides predominantly in the measured $(A_b/A_f)_i$.

(*A*) *Linear pBR322 DNA.* The exponential factors in eq 8 and 9 are set to 1.0, and the equilibrium constants K and K_E' are regarded as adjustable parameters, which are estimated by least-squares as follows. Trial values of K and K_E' are selected. For each chl/bp ratio x_i, the corresponding theoretical ratio $(A_b/A_f)_i{}^{th}$ is calculated by first solving eq 9 for r and then substituting that in eq 8. The sum of the squares of the differences between the measured and theoretical ratios is then calculated according to

$$S = \sum_{i=1}^{N}[(A_b/A_f)_i{}^{exp} - (A_b/A_f)_i{}^{th}]^2 \tag{10}$$

Both K and K_E' are varied systematically until a minimum value of S is obtained, at which point the optimum values of K and K_E' are noted. At small chloroquine binding ratios ($r \ll 1$), A_b/A_f is largely independent of r, as is clear from eq 7, so that the data at small x (or r) contribute virtually nothing to the determination of K. Thus, the optimum chloroquine binding constant K applies only for comparatively high binding ratios $r \geq 0.06$. The optimum value of K for linear DNA is presented in Table III along with computed values for the binding ratio r, the fraction of nonexcluded sites $F = (1 - 2r)^2/(1 - r)$, and both theoretical and measured values of A_b/A_f.

Table III: Least-Squares Binding Parameters for Linear pBR322 DNA in 0.1 M NaCl, $K = 3.81 \times 10^2$ M^{-1}, $K_E' = 2.28 \times 10^5$ M^{-1}, $C_{bp} = 4.04 \times 10^{-5}$ M

x (chl/bp)	r[a]	F[b]	$(A_b/A_f)^{th}$[c]	$(A_b/A_f)^{exp}$	σ_A[d]
0	0			10.8	0.7
0.005	7.58×10^{-5}	0.9998	9.20	10.4	2.1
0.01	1.52×10^{-4}	0.9995	9.20	9.6	0.8
0.04	6.05×10^{-4}	0.9982	9.19	9.1	0.5
0.2	3.01×10^{-3}	0.9910	9.12	9.7	0.2
0.5	7.41×10^{-3}	0.9778	9.00	9.2	0.7
1.0	1.45×10^{-2}	0.9567	8.81	9.7	1.4
5.0	6.22×10^{-2}	0.8177	7.53	8.3	1.3
25.0	1.86×10^{-1}	0.4857	4.47	4.3	0.2
100	3.13×10^{-1}	0.2039	1.88	1.10	0.06

[a] Computed from eq 9. [b] $F = (1 - 2r)^2/(1 - r)$ is the fraction of nonexcluded sites. [c] Computed from eq 8. [d] Standard deviation in $(A_b/A_f)^{exp}$.

Although chloroquine binds predominantly as the doubly charged speices chl^{2+}, the singly charged and neutral species are also present in solution. In general, the total concentration of all species of free chloroquine is

$$C = [\text{chl}^{2+}]\left(1 + \frac{K_1}{[H^+]} + \frac{K_1K_2}{[H^+]^2}\right)$$

where $pK_1 = 8.1$ and $pK_2 = 10.16$ (Cohen & Yielding, 1965) for dissociation of the first and second protons, respectively. The *apparent* equilibrium binding constant K for *total* free chloroquine (all species) is related to the equilibrium binding constant K_{2+} for the doubly charged species by

$$K = K_{2+}/(1 + K_1/[H^+] + K_1K_2/[H^+]^2) \tag{11}$$

K_{2+} is independent of $[H^+]$, but K depends on pH and will at times bear a subscript to denote that. From the measured value $K_{8.5} = 381$ M^{-1} at pH 8.5, we calculate $K_{2+} = 1360$ M^{-1}. The corresponding values of K_{2+} calculated by using eq 11 from published binding data of Jones et al. (1980), Delben et al. (1982), and Stoller and Levine (1963) under similar conditions of temperature and ionic strength range from $K_{2+} = 780$ to 1600 M^{-1}. In our experiment only those (presumably intercalated) chloroquine molecules that compete with ethidium are counted as bound, while those that bind in noncompetitive manner have almost no effect on the analysis, because the vast majority of chloroquine is free. In a sense, this gives the true *intercalation* binding constant.

Equation 11 can be used with the value $K_{2+} = 1360$ M^{-1} to calculate K_{pH} for any other pH under the same conditions of temperature and ionic strength. For example, in analyzing our data for the high-twist supercoiled DNA, we use $K_{7.5} =$

Table IV: Least-Squares Binding Parameters for Normal-Twist Supercoiled pBR322 DNA in 0.1 M NaCl, $E_T = 360^a$, $K_E' = 1.42 \times 10^5$ M^{-1}, $C_{bp} = 7.34 \times 10^{-5}$ M

x (chl/bp)	r^b	F^c	$(A_b/A_f)^{th\,d}$	$(A_b/A_f)^{exp}$	$\sigma_A{}^e$
0	0		13.2	0.51	
0.01	2.90×10^{-4}	0.9991	13.18	12.9	2.5
0.1	2.85×10^{-3}	0.9915	13.00	15.2	1.4
1.0	2.57×10^{-2}	0.9237	11.45	13.2	2.1
10.0	1.41×10^{-1}	0.6023	5.62	7.60	0.76
50.0	2.72×10^{-1}	0.2852	1.93	1.92	0.03

[a] Determined by using $K = 381$ M^{-1}, as described in text. [b] Computed from eq 8. [c] $F = (1 - 2r)^2/(1 - r)$ is the fraction of nonexcluded sites. [d] Computed from eq 9. [e] Standard deviation in $(A_b/A_f)^{exp}$.

Table V: Least-Squares Binding Parameters for High-Twist Supercoiled pBR322 in 0.1 M NaCl, $E_T = 460^a$, $K_E' = 4.45 \times 10^5$ M^{-1}, $C_{bp} = 2.98 \times 10^{-5}$ M

x (chl/bp)	r^b	F^c	$(A_b/A_f)^{th\,d}$	$(A_b/A_f)^{exp}$	$\sigma_A{}^e$
0	0		22.6	6.3	
0.1	3.94×10^{-3}	0.9882	22.06	17.6	4.2
0.5	1.83×10^{-2}	0.9454	20.17	27.2	2.5
2.0	5.93×10^{-2}	0.8257	15.50	21.4	4.9
4.0	9.64×10^{-2}	0.7210	12.04	15.7	1.8
6.0	1.23×10^{-1}	0.6473	9.93	14.3	3.1
10.0	1.61×10^{-1}	0.5469	7.45	9.03	2.31
15.0	1.94×10^{-1}	0.4657	5.73	8.36	2.73
20.0	2.17×10^{-1}	0.4095	4.69	5.89	0.85
30.0	2.49×10^{-1}	0.3348	3.46	3.25	0.16
50.0	2.89×10^{-1}	0.2513	2.30	2.25	0.31

[a] Determined by using $K = 1088$ M^{-1}, as described in text. [b] Computed from eq 9. [c] $F = (1 - 2r)^2/(1 - r)$ is the fraction of nonexcluded sites. [d] Computed from eq 8. [e] Standard deviation in $(A_b/A_f)^{exp}$.

1088 M^{-1} as the apparent intrinsic equilibrium constant for total free chloroquine.

(B) Supercoiled DNA. The fixed parameters are as follows. The apparent intrinsic equilibrium constant K for chloroquine binding is assumed to have the value $K_{7.5} = 1088$ M^{-1} or $K_{8.5} = 381$ M^{-1}, as determined for the linear pBR322 DNA at the appropriate pH. The unwinding angles are taken to be $\phi_E = -26°$ for ethidium (Wang, 1974) and $\phi = -17°$ for chloroquine (Jones et al., 1980). We also take $r^* = -\Delta l(360)/(17)(4363)$ and $r_E^* = -\Delta l(360)/(26)(4363)$, where Δl is the linking-number difference, as shown in Appendix A. For the normal-twist supercoiled DNA we take $\Delta l = -20$, hence $r^* = 0.097$, and for the high-twist supercoiled DNA, we take $\Delta l = -35$, hence $r^* = 0.170$.

The adjustable parameters are K_E' and the twist energy parameter E_T. First a trial value of E_T is selected, from which the quantities a, a_{EC}, and $a_E = 2E_T(\phi_E/360)^2$ are calculated. Then K_E' is determined directly from the measured ratio A_b/A_f *in the absence of chloroquine* by using the relation

$$A_b/A_f = K_E' \exp[a_E r_E^*] \qquad (12)$$

which follows from eq 4 for the binding of ethidium *in the absence of chloroquine*, when $a_E r_E \ll a_E r_E^* < 1.0$, as is the case here. Then, for each nonzero chl/bp ratio x_i, the corresponding theoretical ratio $(A_b/A_f)_i^{th}$ is calculated by first solving eq 9 for r and then substituting that into eq 8. Again, the quantity S in eq 10 is calculated, and E_T is varied systematically until the minimum value of S is obtained. The measured and best-fit theoretical ratios A_b/A_f for the normal-twist and high-twist supercoiled DNAs are listed along with other pertinent parameters in Tables IV and V, and the optimum twist energy parameters are listed in Table II.

Results

(A) Linear pBR322 DNA. Except at the very highest chl/bp ratios (25 and 100) the decay of the fluorescence intensity exhibits a dominant component with a lifetime $\tau = 21.5 \pm 1.0$ ns, corresponding to normally intercalated ethidium, and a small amplitude of fast component with a lifetime $\tau \cong 2 \pm 1$ ns, corresponding to free (nonintercalated) ethidium. The ratio A_b/A_f of the decay amplitudes associated with intercalated and free ethidium is plotted vs (chl/bp) in Figure 1. A_b/A_f is essentially independent of chloroquine concentration at least up to chl/bp = 5. Higher chloroquine concentrations evidently force the ethidium off the DNA. When chl/bp = 100, the ethidium fluorescence decay requires three exponentials with lifetimes of 22, 5, and 1 ns. The 5-ns component probably represents an incompletely intercalated binding site.

The best-fit theoretical curve for the amplitude ratio $(A_b/A_f)^{th}$ is shown in Figure 1. The corresponding binding ratios r at each value of chl/bp are presented in Table III along with $(A_b/A_f)^{exp}$, $(A_b/A_f)^{th}$, the fraction F of nonexcluded sites, the experimental standard deviation σ_A, and the optimum apparent binding constant. The fit is good, and agreement of the implied equilibrium constant K_{2+} with the values obtained from other published data is satisfactory, as noted under *Chloroquine Binding Parameters* above.

The best-fit torsion constant α is independent of the time span of the data for all chl/bp ≤ 25. One may infer that the torsional rigidity is uniform over distances of at least 1000 base pairs under these conditions. For chl/bp ≤ 25, the initial anisotropy is essentially constant at $r_0 = 0.33 \pm 0.02$. At chl/bp = 100, the torsion constant for the 0–40-ns time span ($\alpha = 16 \times 10^{-12}$ dyn·cm) is very large and falls to a lower but still high value ($\alpha = 8 \times 10^{-12}$ dyn·cm) for the 0–120-ns time span. Thus, the apparent torsion constant is nonuniform and rather high. Also at chl/bp = 100, the initial anisotropy is anomalously low, in the range $r_0 = 0.25$–0.28 for the 0–40-, 0–80-, and 0–120-ns time spans. The dynamics and very likely also the structure of this linear DNA are evidently strongly perturbed when chl/bp = 100.

Average torsion constants are computed from the values obtained for the 40-, 80-, and 120-ns time spans and plotted vs chl/bp ratio in Figure 1. The magnitude as well as the uniformity of the torsion constant is evidently unaffected by the intercalation up to the point (chl/bp = 25) where the ethidium probe dye is being forced off the DNA. The initial anisotropy also remains essentially constant over the same range. At higher chl/bp ratio (≥ 25) the intercalated chloroquine evidently has a substantial effect on the DNA dynamics and/or structure, but a detailed assessment is difficult due to the dissociation of ethidium from the DNA.

(B) Normal-Twist Supercoiled pBR322 DNA. The results here are similar to those obtained for linear pBR322 DNA. For chl/bp ≤ 10 the fluorescence decay exhibits a dominant normal component with $\tau_f = 21.5 \pm 1.0$ ns and a small amplitude of fast component with $\tau_f = 2 \pm 1$ ns. The ratio A_b/A_f of the decay amplitudes associated with the normal (intercalated) and fast (free) components is plotted vs chl/bp ratio as the triangles in Figure 2. This ratio remains roughly constant up to chl/bp = 1.0 and falls off at higher chl/bp nearly in parallel with the linear DNA. When chl/bp = 50, the fluorescence decay requires three components with τ = 1, 5, and 22 ns.

The best-fit theoretical curve for the amplitude ratio $(A_b/A_f)^{th}$ is shown as the dotted line in Figure 2. The corresponding binding ratios r at each value of chl/bp are presented in Table IV along with $(A_b/A_f)^{exp}$, $(A_b/A_f)^{th}$, F, σ_A, and the optimum value $E_T = 360$ of the twist energy parameter. The fit is acceptable. There is certainly no indication

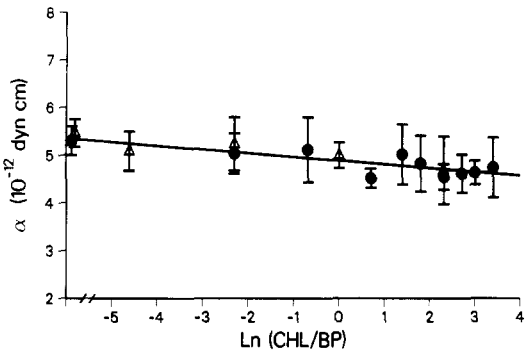

FIGURE 3: Experimental torsion constants α for supercoiled pBR322 DNAs vs added chloroquine per base pair (chl/bp). Data for normal-twist ($\sigma = -0.048 \pm 0.005$) supercoiled DNA are denoted by triangles. Data for high-twist ($\sigma = -0.083 \pm 0.007$) supercoiled DNA are denoted by solid circles. Solution conditions are the same as in Figure 2.

that the binding theory is fundamentally inadequate.

The best-fit torsion constant is independent of the time span for all chl/bp $\leq$ 10. Average torsion constants are computed from measurements on all three time spans, as for the linear DNA. These average α values are plotted vs chl/bp ratio as the triangles in Figure 3. For the normal-twist supercoiled conformation, the torsion constant exhibits a significant though modest decrease up to the point where the ethidium is being forced off the DNA. Up to chl/bp = 10 the initial anisotropy remains essentially constant at $r_0 = 0.33 \pm 0.02$. Intercalated chloroquine evidently alters the torsional dynamics and rigidity of this supercoiled DNA.

At chl/bp = 50 the apparent torsion constant of this supercoiled DNA falls from a very high value, 8.8×10^{-12} dyn·cm, at 36-ns time span to a very low value, 3.7×10^{-12} dyn·cm, at 110-ns time span, which indicates a highly nonuniform torsional rigidity that is anomalously weak over long distances. Also, the initial anisotropy rises from an anomalously low value 0.27 up to above the normal range for this DNA. In contrast, the linear DNA exhibits no sign of anomalously low torsion constant for any time span, even at chl/bp = 100. One may conclude that the dynamics and/or the structure of the supercoiled DNA are substantially altered at chl/bp = 50, but in a different way from the alteration of linear DNA at chl/bp = 100.

(*C*) *High-Twist Supercoiled pBR322 DNA.* The results here are similar to those obtained for linear and normal-twist supercoiled pBR322 DNAs. For chl/bp $\leq$ 10, the fluorescence decay exhibits a dominant normal component with $\tau_f = 21.5$ ns and a small amplitude of fast component with $\tau_f = 2 \pm 1$ ns. The ratio A_b/A_f of the decay amplitudes associated with the normal (intercalated) and fast (free) components is plotted vs chl/bp as squares in Figure 2. This ratio remains (roughly) constant up to chl/bp = 1.0 and falls off at higher chl/bp nearly parallel with the linear and normal-twist supercoiled DNAs. When chl/bp $\geq$ 50, the fluorescence decay requires three (or more) components with τ = 1, 2–10, and 22 ns.

The best-fit theoretical curve for the amplitude ratio $(A_b/A_f)^{th}$ is shown as the solid line in Figure 2. The corresponding ratios r at each value of chl/bp are presented in Table V along with $(A_b/A_f)^{exp}$, $(A_b/A_f)^{th}$, F, σ_A, and the optimum value $E_T = 460$ of the twist energy parameter. The fit is acceptable in view of the large uncertainties in the experimental ratios at low chl/bp ratios.

The best-fit torsion constant is independent of time span (40, 80, and 120 ns) for all chl/bp $\leq$ 30. Average torsion constants computed from measurements on all three time spans are plotted vs chl/bp ratio in Figure 3. For the high-twist supercoiled pBR322 DNA, the torsion constant exhibits a significant though modest decrease up to chl/bp = 30, but the initial anisotropy remains essentially constant at $r_0 = 0.33 \pm 0.02$. Evidently, intercalated chloroquine alters the torsional dynamics and rigidity of this DNA.

At chl/bp = 50, the torsion constant is highly nonuniform, ranging from about 7×10^{-12} dyn·cm at 40 ns to about 3.4×10^{-12} dyn·cm at 120 ns. Though qualitatively similar to what is observed for the normal-twist supercoiled DNA, this behavior is less extreme, presumably because the high-twist supercoiled DNA is not as positively twisted at this point. Nonetheless, the torsion constant on the longest time span falls below the normal value, in contrast to the behavior observed for linear DNA. This lends support to the notion that the structural alterations wrought by very high levels of chloroquine binding in linear and supercoiled DNAs must be significantly different.

(*D*) *Anharmonicity of the Torsion Potential.* In the absence of chloroquine, the torsion constants of all three DNAs are virtually identical, $\alpha = (5.0 \pm 0.4) \times 10^{-12}$ dyn·cm. Up to the level of static twist in the high-twist supercoiled DNA, we find no evidence of anharmonicity of the torsion potential. However, other observations (Song et al., 1988) indicate that superhelical stress may induce allosteric transitions, in which case the secondary structures of supercoiled and linear DNAs might not be identical, despite their similar torsion constants.

(*E*) *Twist-Energy Parameters.* The twist energy parameters for ethidium binding to normal-twist and high-twist supercoiled pBR322 DNAs are determined from the competitive dialysis results, as described under *Competitive Dialysis* above. The twist energy parameters for chloroquine binding to normal-twist and high-twist supercoiled DNAs are determined by fitting the A_b/A_f ratios of the ethidium fluorescence, as described under *Chloroquine Binding Parameters*. These twist energy parameters are all displayed in the lower portion of Table II.

Discussion and Conclusions

FPA and Torsion Constant. (*A*) *Linear pBR322 DNA.* For linear DNA, the FPA decay remains invariant and the torsion constant α remains essentially uniform and constant up to a chl/bp ratio of 25, which corresponds to a binding ratio r = 0.19 (cf. Table III). This is 40% of the saturation binding, which occurs at $r = 0.5$ in the nearest-neighbor exclusion model. This finding argues strongly that neither the FPA decay nor the Brownian torsional deformations are significantly influenced by diffusion of kinks or solitons, which should be strongly affected by such extensive intercalation. We can now state that the FPA decay and the magnitude and uniformity of the torsion constant α are unaffected by (1) T from 0 to 70 °C (Thomas & Schurr, 1983; Wilcoxon & Schurr, 1983; Shibata, unpublished data), (2) GC composition from 34 to 100% (Fujimoto et al., 1985), (3) spermidine binding in 10 mM NaCl up to about 85% neutralization of the phosphate charge (at neutral pH) (Wilcoxon et al., 1982), and (4) intercalation of chloroquine up to $r = 0.19$. These observations, together with the observed uniformity of α, are difficult to reconcile with any model in which the FPA decay and Brownian torsional deformations occur predominantly at structural aberrations of any kind, whether kinks, locally denatured regions, or whatever, because the equilibrium populations and dynamics of such structures would be expected to be strongly perturbed by one or more of these agents. All these data are consistent with the notion that Brownian torsional deformations proceed predominantly by gradual deformations of the native secondary structure.

In order to set quantitative limits on the apparent torsion constant between the intercalated chloroquine and its neighboring base-pairs, we proceed as follows. The torsion normal mode with relaxation time τ has a wavelength $\lambda = \pi/\arcsin[(\gamma/4\alpha\tau)^{1/2}]$ (Allison & Schurr, 1979). Using $\alpha = 5.0 \times 10^{-12}$ dyn·cm, one finds $\lambda = 57$ bp for $\tau = 1$ ns and $\lambda = 80$ bp for $\tau = 2$ ns, etc. Thus, our FPA technique monitors normal modes with wavelengths of 57 base pairs or more. When the wavelengths being probed are all much greater than the average spacing between bound intercalators, the dynamics should be governed by the effective long-range torsional rigidity C defined by Wilcoxon and Schurr (1983) (cf. their eq A33 and A34). One may define the corresponding effective long-range torsion constant using the relation $\alpha_{eff} = C/h$, where $h = 3.4 \times 10^{-8}$ cm is the rise per base pair. For a filament comprising two kinds of Hookean torsion springs with small rms displacements, one obtains

$$\alpha_{eff} = \alpha_0 \frac{1}{(1-f) + f(\alpha_0/\alpha_d)} \qquad (13)$$

wherein $(1-f)$ is the fraction of normal springs with torsion constant α_0 and f is the fraction of different springs with torsion constant α_d. When $r = 0.2$, there is one intercalated chloroquine for every 5 base pairs. The DNA is imagined to consist of translationally repeated unit cells comprising six subunits, namely, 5 base pairs and 1 intercalator, and also their six springs (to the right of each subunit). Of these six springs, four represent interactions between two base pairs and have torsion constant $\alpha_0 = 5.0 \times 10^{-12}$ dyn·cm, and two represent interactions between the intercalated chloroquine and a base pair and have torsion constant α_d. For $r = 0$ the measured torsion constant corresponds to α_0, and for $r = 0.2$, the measured torsion constant corresponds to α_{eff} with $f = 2/6$. Our data confirm that α_{eff} and α are the same within the experimental error of about 10%. We can say with some confidence that α_{eff} does not differ from α_0 by more than 15%, whence $0.85 \leq \alpha_{eff}/\alpha_0 \leq 1.15$. This statement in conjunction with eq 13 imposes upper and lower limits on the ratio α_d/α_0, namely, $0.65 \leq \alpha_d/\alpha_0 \leq 1.64$. Thus, with some confidence we can say that the apparent torsion constant α_d between intercalated chloroquine and a base pair is not smaller than α_0 by more than 35%, not larger than α_0 by more than 64%, and is most probably nearly the same as α_0. In view of these limits one may conclude that either (a) the chloroquine intercalation site does not correspond to a Sobell β-kink or (b) the torsion constant of the Sobell β-kink is not smaller than the torsion constant between base pairs by as much as a factor of 2 and may not be smaller at all. In either case the predictions of Sobell et al. (1983) are found not to apply to intercalated chloroquine. The limits on α_d also rule out any greatly enhanced torsion constant between an intercalated chloroquine and its neighboring base pairs. The hypothesis of Hogan and Jardetzky (1980) that the intercalated dye is rigidly clamped to its neighboring base pairs evidently is not valid for bound chloroquine. In a forthcoming paper it will be shown that similar conclusions hold for ethidium.

At chl/bp 100, corresponding to $r = 0.315$ (or 63% saturation) the apparent torsion constant becomes nonuniform and exhibits a rather high value. This could arise from ethidium-binding sites in which the transition dipole makes a smaller polar angle with the helix axis, from ethidiums distributed throughout heterogeneous regions with substantially stiffer secondary structure, from self-cross-linking of the duplex filaments by the doubly charged chloroquine, or possibly from other mechanisms.

(*B*) *Supercoiled pBR322 DNAs.* In the absence of chloroquine the apparent torsion constants of the normal-twist and high-twist supercoiled DNAs are uniform and are essentially identical with that of the linear DNA, $\alpha = (5.0 \pm 0.4) \times 10^{-12}$ dyn·cm. However, these torsion constants decrease progressively by about 15% with increasing chl/bp ratios up to 10 and 30 for respectively the normal-twist and high-twist supercoiled DNAs. For the normal-twist sample, the ratio chl/bp = 10 corresponds to a binding ratio $r = 0.141$ (cf. Table IV), or 28% of saturation binding in the nearest-neighbor exclusion model. The effective superhelix density of the normal-twist DNA at $r = 0.141$ is $\sigma = (r - r^*)(17/360)(10.4) = +0.022$, which is obtained by using $r^* = 0.097$. Likewise, for the high-twist sample, the ratio chl/bp = 30 corresponds to $r = 0.249$ (cf. Table V), or 50% of saturation binding. The effective superhelix density of the high-twist supercoiled DNA at $r = 0.249$ is $\sigma = +0.039$, which is obtained by using $r^* = 0.170$. Thus, for both supercoiled DNAs, the effect of intercalated chloroquine to reduce the apparent torsion constant persists through the $\sigma = 0$ region up to substantial positive superhelix density. For the normal-twist DNA, $\sigma = 0$ occurs when $r = r^* = 0.097$ and chl/bp = 4.9 (from eq 9). For the high-twist DNA, $\sigma = 0$ occurs when $r = r^* = 0.170$ and chl/bp = 10.2.

At the chl/bp ratio where $\sigma = 0$, not only should superhelical strain be absent but also the binding ratio $r = r^*$ of the supercoiled DNA should match that of the linear DNA at the same concentration (cf. eq 9). Thus, supercoiled DNA/chloroquine complexes with $\sigma = 0$ should be locally identical with the corresponding linear DNA/chloroquine complexes and therefore should exhibit the same FPA dynamics. This is quite contrary to our observations! Although the difference in α between the supercoiled and linear DNA/chloroquine complexes is not large, it is nonetheless statistically significant. Our confidence that this difference is real is bolstered by the observation of even larger differences when other dyes (Wu et al., 1988) including ethidium (Fujimoto et al., 1988) are used. A 15% reduction in apparent α could arise from any of the following causes: (1) a 15% decrease in (actual) torsion constant; (2) a much larger relative decrease in bending rigidity; (3) a change in the tilt angle of the ethidium from 70.5° to 90°; (4) a clustering of the ethidium, so that excitation transfer contributes significantly to the depolarization process. In any case, it is clear that the local structure or rigidity in our supercoiled DNA/chloroquine complexes with $\sigma = 0$ must differ in some fundamental way from their corresponding linear counterparts with the same binding ratios. Although this confirms that there is some flaw in our understanding of relaxed supercoiled DNA/dye complexes, it does not provide an immediate explanation for the discrepancy between the twist energy parameters obtained by the ligation method and by dye-binding methods. Of the various possibilities indicated above, only a large relative decrease in bending rigidity could cause the observed 2-fold reduction in E_T.

A tentative explanation for the inequivalence of linear and supercoiled DNA/chloroquine complexes and for the discrepancy in E_T values will be presented in a subsequent publication, where additional pertinent experimental results will be presented.

Limits on the ratio α_d/α_0 are found in the same way as for linear DNA. For the high-twist supercoiled DNA at $r = 0.249$, α_{eff}/α_0 has a most probable value of 0.85 and lies in the range $0.70 \leq \alpha_{eff}/\alpha_0 \leq 1.0$. We find that α_d/α_0 lies in the range $0.52 \leq \alpha_d/\alpha_0 \leq 1.0$ with a most probable value $\alpha_d/\alpha_0 = 0.65$. It is assumed in this analysis that the decrease in α_{eff} is due only to a decreased α_d between chloroquine and a base

pair. However, it is likely that α_0 is also decreased for these supercoiled DNAs, as suggested above, so this analysis may be irrelevant.

At chl/bp = 50, corresponding to $r = 0.272$ (54% of saturation), the apparent torsion constant of the normal-twist supercoiled DNA becomes highly nonuniform and falls from a very high value for short time spans to a very low value for the longest time span (0–120 ns). The high values observed for the short time spans might be associated with a 5-ns component in the decay of the fluorescence intensity, as noted also for the linear DNA at chl/bp = 100. However, the low torsion constant ($\alpha \cong 3.5 \times 10^{-12}$ dyn·cm) observed for supercoiled DNA on the longest time span differs markedly from the somewhat high value ($\alpha \cong 8 \times 10^{-12}$ dyn·cm) observed for linear DNA, also on the longest time span. This very likely reflects a substantial structural difference between the supercoiled and linear DNA that is induced by high levels of intercalation. This may be related to the superhelix density, which is large and positive ($\sigma = 0.086$) for $r = 0.272$.

At chl/bp = 50, corresponding to $r = 0.289$ (58% of saturation), the apparent torsion constant of the high-twist supercoiled DNA becomes highly nonuniform and falls from 7×10^{-12} dyn·cm on the 40-ns time span to 3.4×10^{-12} dyn·cm on the 120-ns time span. This very likely reflects the onset of structural differences at the positive superhelix density ($\sigma = 0.058$) for $r = 0.289$.

It is notable that both linear and supercoiled DNAs undergo marked changes when $r \geq 0.27$, although the changes in α (on the longest time span) are in opposite directions for the linear and supercoiled species.

(C) Twist Energy Parameters. The twist energy parameters determined for chloroquine binding to normal-twist ($E_T = 360$) and high-twist ($E_T = 460$) supercoiled pBR322 DNAs lie somewhat below the consensus dye-binding range ($E_T = 500 \pm 60$). Our values apply to fairly high added chloroquine levels (chl/bp $\geq$ 5). The effective superhelix density of the normal-twist and high-twist supercoiled DNAs passes from negative to positive values near chl/bp = 4.9 and 10.2, respectively, so the twist energy parameters for chloroquine binding are determined largely in the region of positive supercoiling.

The twist energy parameters determined for ethidium binding to normal-twist ($E_T = 280$) and high-twist ($E_T = 345$) supercoiled pBR322 DNAs similarly lie below the consensus dye-binding range. In this case, the values apply for relatively low levels of dye binding. E_T values determined for ethidium binding to each DNA are close to 75% of the values determined for chloroquine binding to the same DNA.

The present results show that the twist energy parameters of our supercoiled pBR322 DNAs in 0.1 M NaCl lie well below the reported ligation values for pBR322 DNA in 60 mM NaCl. It is evident that the large difference between twist energy parameters obtained by ligation and dye-binding methods cannot be generally attributed to much higher NaCl concentrations prevailing in the dye-binding experiments (cf. Table II).

The twist energy parameters determined for normal-twist supercoiled pBR322 DNA, by use of either ethidium or chloroquine, are about 20% lower than those obtained for the high-twist DNA. This effect of superhelix density on E_T does not reflect a difference in torsional rigidity but must be associated with a difference in the bending rigidity in the prevailing type of tertiary structure, either of which could alter the effective "force" constant for supercoiling, or with some other difference.

The low values of E_T obtained from ethidium-binding studies cannot simply be ascribed to anomalous behavior of that particular intercalator because chloroquine binding also yields E_T values in a comparably low range.

We do not understand why our E_T values obtained from ethidium binding are significantly lower than other reported values. It is notable that our lowest value ($E_T = 280 \pm 70$) was determined at a much lower binding ratio ($r = 0.0025$) than is normally investigated. Our salt concentration is also lower than that of most previous ethidium-binding determinations of E_T.

There are important differences between the ligation method and dye-binding methods. In the former, only states accessible by thermal fluctuation from the relaxed condition are generated. Thus, the ligation method samples only states near the normal B conformation. Also, in this method the individual topoisomers are resolved and quantitated to determine their relative concentrations. In contrast, the dye-binding method samples a very much wider range of superhelix densities, over which allosteric transitions in secondary structure may occur. Moreover, they reflect merely the *average* behavior of a population of different topoisomers. At a given concentration of free dye, each topoisomer (i) should obey the relation

$$r_i/C = K \exp[a(r_i^* - r_i)](1 - 2r_i)^2/(1 - r_i) \quad (14)$$

where $r_i^* = (\Delta l)_i(360)/\phi N$ depends on the particular linking-number difference and $a = 2E_T(\phi/360)^2$. The average isotherm for a collection of topoisomers is then

$$\frac{\bar{r}}{C} = \sum_i f_i \frac{r_i}{C} \quad (15)$$

where f_i is the fraction of DNA molecules comprising each topoisomer. For an equilibrium population of topoisomers, eq A19 and A20 give

$$f_i = \exp[-(E_T/N)(\Delta l)_i^2] / \sum_j \exp[-(E_T/N)(\Delta l)_j^2] \quad (16)$$

We have estimated the effect of a distribution of topoisomers on the dye-binding results in the following way. A value of E_T is selected, and $\exp[-(E_T/N)(\Delta l_m)^2]$ is calculated for the median linking-number difference Δl_m and for the consecutive linking numbers on either side until this exponential quantity falls below 1% of that for Δl_m. This set of linking-number differences defines the collection of topoisomers and is used for normalization in the denominator in eq 16. The f_i are calculated for this set of topoisomers. By use of eq 14, r_i for each topoisomer in the set can be determined for any given value of C. Then by use of eq 15, $\bar{r}/C$ is calculated for various values of C and plotted vs $\bar{r}$. This curve is now treated as "experimental" data and analyzed by using eq 4, with r^* calculated for the median linking-number difference and a (or E_T) now taken as an adjustable parameter. If $E_T = 1000$ is used to construct the experimental curve for the collection of topoisomers, then the value $E_T = 890$ is recovered from the analysis. The set comprises 13 topoisomers in this case. If, instead, $E_T = 500$ is used to construct the experimental curve, the distribution of topoisomers is twice as broad, and the value $E_T = 377$ is recovered from the analysis. From these results, we conclude that the distribution of topoisomers cannot account for mose of the substantial differences between values of E_T obtained by the ligation method and by the dye-binding method.

It is conceivable that the Mg^{2+} present in the ligation buffer could affect the rigidities and twist energy parameter. We have examined this possibility by measuring the torsion constant of a largely relaxed (nicked) pBR322 DNA using

standard FPA techniques in the same buffer with [Mg^{2+}] from 0 to 40 mM, at which point the ethidium is significantly displaced from the DNA. A 15% decrease in torsion constant was observed over this range. Therefore, it seems most unlikely that Mg^{2+} could be the cause of the higher twist energy parameter observed in the ligation experiments.

We conclude that the discrepancy in E_T values between ligation and dye-binding experiments cannot simply be ascribed to any singular behavior of ethidium, to different ambient salt concentrations, to the presence of Mg^{2+} in the case of ligation, or to averaging over a distribution of topoisomers in the case of dye binding. This discrepancy is almost certainly linked to the observation that supercoiled DNA/chloroquine complexes with $\sigma = 0$ are not equivalent in local rigidity and/or structure to linear DNA/chloroquine complexes with the same amount of intercalated chloroquine.

Appendix A: Statistical Thermodynamics of Supercoiled DNAs and Their Complexes with Intercalating Dyes

Our objectives here are twofold. First, we establish the connections among (1) the elementary torsion constant α that governs the twisting motions of DNA and that is manifested in FPA experiments; (2) the effective torque constant for fluctuations in *net* twist of a supercoiled DNA; and (3) the twist energy parameter E_T for the free energy of supercoiling. Then we shall treat the effect of intercalating dyes on the free energy of supercoiling. The former objective has been examined by using simulation methods by Vologodskii et al. (1979), Le Bret (1979, 1980, 1984), and Levene and Crothers (1986). Using an appropriate assumption (eq A12), we obtain analytical, though incomplete, results.

Free Energy of Supercoiling. Consider a circular DNA containing N base-apirs, labeled 1, ..., N, each of which is represented by a disk. Each disk is assumed to be connected to its successor by a Hookean torsion spring with torsion constant α, and a Hookean bending spring with bending constant κ_β. In each disk is fixed a coordinate frame with the z axis taken along the symmetry axis of the disk. The Euler transformation that carries the coordinate frame of the i disk into that of the $(i + 1)$ disk is $\Phi_{i,i+1} = (\alpha_{i,i+1}\beta_{i,i+1}\gamma_{i,i+1})$. The twist in radians from one disk to the next is defined by

$$\phi_{i,i+1} = (\alpha_{i,i+1} + \gamma_{i,i+1}) \tag{A1}$$

The potential energy of this model molecule is assumed to be given by the Hookean form

$$U = \frac{\kappa_\beta}{2}\sum_{i=1}^{N}\beta_{i,i+1}{}^2 + \frac{\alpha}{2}\sum_{i=1}^{N}(\phi_{i,i+1} - \phi_0)^2 \tag{A2}$$

where ϕ_0 (approximately 36°) is the equilibrium twist from one disk to another *in an unstrained molecule.* The first term is the bending potential U_b, and the second is the twisting potential, U_t. The net twist in radians of the entire molecule is defined by

$$t \equiv \sum_{i=1}^{N}\phi_{i,i+1} \tag{A3}$$

The twisting potential in eq A2 can be written as

$$U_t = \frac{\alpha}{2}\sum_{i=1}^{N}(\phi_{i,i+1} - t/N)^2 + \frac{\alpha}{2N}(t - t_0)^2 \tag{A4}$$

where $t_0 = N\phi_0$ is the equilibrium net twist *in an unstrained molecule.* The *minimum* twist energy in a *strained* molecule with net twist t occurs when $\phi_{i,i+1} = t/N$ for all springs, in which case $U_t = (\alpha/2N)(t - t_0)^2$. Thus, the *minimum* twist energy of a strained molecule is quadratic in the twist difference $t - t_0$, and the effective force constant is α/N. At a finite temperature, the system will exhibit fluctuations in twist of the individual springs, as well as in the net twist, and these fluctuated state contribute to the free energy.

Define the vector from the center of the i disk to the center of the $(i + 1)$ disk as the bond vector $\mathbf{b}_i$. The writhe of that bond vector is defined by (Fuller, 1971; Levene & Crothers, 1986)

$$w_i = \frac{|\mathbf{b}_i|^2}{4\pi}\sum_{j\neq i}\frac{1}{|\mathbf{r}_j - \mathbf{r}_i|^2}(\mathbf{t}_i \times \mathbf{e}_{ij})\cdot\mathbf{t}_j \tag{A5}$$

where $\mathbf{r}_i$ and $\mathbf{r}_j$ denote positions of the (centers of the) bond vectors, $\mathbf{t}_i \equiv \mathbf{b}_i/|\mathbf{b}_i|$ is the unit vector along the ith bond vector, and $\mathbf{r}_{ij}$ is the unit vector from the ith bond vector to the jth. The net writhe is

$$w = \sum_{i=1}^{N} w_i \tag{A6}$$

Again, at a finite temperature, a closed circular DNA will exhibit fluctuations in the writhe of the individual bond vectors, as well as in the net writhe, and these fluctuated configurations contribute to the free energy.

The partition function for a DNA with net writhe w and net twist t is

$$Z(t,w) = \int\cdots\int\prod_{i=1}^{N}\{d\alpha_{i,i+1}\, d\beta_{i,i+1} \sin\beta_{i,i+1}\, d\gamma_{i,i+1}\} \times \exp[-(U_b + U_t)/k_BT]\ \delta(w - \sum_{j=1}^{N} w_j)\delta(t - \sum_{l=1}^{N}\phi_{l,l+1}) \tag{A7}$$

wherein U_b and U_t correspond to the first and second terms in eq A2 and the δ-functions are inserted to enforce the constraints on net writhe and net twist. The writhe constraint depends on the set of angles $\{\alpha_{i,i+1}, \beta_{i,i+1}, i = 1, ..., N\}$ but not on the set $\{\gamma_{i,i+1}, i = 1, ..., N\}$, so the integrand factors into a part dependent on the set $\{\alpha_{i,i+1}, \beta_{i,i+1}, i = 1, ..., N\}$ and another part dependent on the set $\{\phi_{i,i+1}, i = 1, ..., N\}$. We introduce the change of variables $(\alpha_{i,i+1}, \beta_{i,i+1}, \gamma_{i,i+1}) \rightarrow (\alpha_{i,i+1}, \beta_{i,i+1}, \mu_{i,i+1})$, where $\mu_{i,i+1} \equiv \phi_{i,i+1} - t/N = (\alpha_{i,i+1} + \gamma_{i,i+1} - t/N)$. The Jacobian of this transformation is 1.0 (for fixed t). The partition function itself now factors to give

$$Z(t,w) = Z_t(t)Z_w(w) \tag{A8}$$

where

$$Z_w(w) \equiv \int\cdots\int\prod_{i=1}^{N}\{d\alpha_{i,i+1}\, d\beta_{i,i+1} \sin\beta_{i,i+1}\} \times \exp[-U_b/k_BT]\delta(w - \sum_{j=1}^{N} w_j) \tag{A9}$$

and

$$Z_t(t) = \exp[-(\alpha/2Nk_BT)(t - t_0)^2] \times \int\cdots\int d\mu_1...d\mu_N\delta(\sum_{j=1}^{N}\mu_j - 0)\exp[-(\alpha/2k_BT)\sum_{i=1}^{N}\mu_i{}^2] = \exp[-(\alpha/2Nk_BT)(t - t_0)^2]q \tag{A10}$$

where

$$q \equiv q(\alpha,N,T) \equiv (2\pi k_BT/\alpha)^{N/2}(2\pi Nk_BT/\alpha)^{-1/2} \tag{A11}$$

The integral in eq A10 can be evaluated by first performing the integral over $d\mu_N$, then expressing the exponent in matrix form, $\mu^\dagger\mathbf{A}\mu/2\sigma^2$, where $\sigma^2 \equiv k_BT/\alpha$ and the elements of the $(N - 1)(N - 1)$ matrix $\mathbf{A}$ are $A_{lm} = 1 + \delta_{lm}$, and finally introducing the unitary transformation $\mathbf{Q}(\det|\mathbf{Q}| = 1.0)$ that diagonalizes $\mathbf{A}$. The first $N - 2$ eigenvalues of $\mathbf{A}$ are 1, and

the last is N. This leads to a product of standard Gaussian integrals, which are readily performed to give eq A10 and A11. The integration can also be accomplished by temporarily setting the zero in the δ-function to the variable s and noting that, except for missing normalization constants, the resulting integral is just the distribution function for the sum s of Gaussian random variables of zero mean with variance σ^2. This distribution is itself a normalized Gaussian with zero mean and variance $\sigma_s^2 = N\sigma^2$. Upon inserting the missing normalization factors and setting $s = 0$, one obtained the result in eq A10 and A11.

It is not yet possible to evaluate $Z_w(w)$ analytically for large N, although it has been simulated by using Monte Carlo techniques by Volodoskii et al. (1979), Le Bret (1979, 1980, 1984), and Levene and Crothers (1986). These workers are not in complete agreement as to the results for short circular DNAs. We note that $Z_w(w)$ is just an unnormalized distribution function for w. We *assume* here that, *for sufficiently large* N, $Z_w(w)$ is given by

$$Z_w(w) = \exp[-(\kappa_w/(2Nk_BT))w^2]r \qquad \text{(A12)}$$

where κ_w should be proportional to κ_β and $r = r(\kappa_\beta,N,T)$ is a function only of the variables indicated. The assumed Gaussian form is justified to some extent by the simulation results and is required in any case to yield agreement with the experimental results. This simple Gaussian form is probably valid only in those cases where a single family of tertiary conformations (e.g., either toroidal or straight interwound) predominates. The effective force constant κ_w undoubtedly depends on the particular dominant tertiary conformation, as does r.

A closed circular DNA obeys the well-known constraint (in radians) (Fuller, 1971)

$$L = 2\pi l = t + w \qquad \text{(A13)}$$

where l is an integral topological constant called the linking number for that particular topoisomer. Imposing the constraint $L = t + w$ gives the partition function for a *closed* circular DNA with constraint L and net writhe w. This can be written in the form

$$Z_L(L - w,w) \equiv Z_t(L - w)Z_w(w) = \exp\left[-\left\{\frac{ak}{2(a + k)}(L - t_0)^2 + \frac{(a + k)}{2}(w - w_0)^2\right\}/k_BT\right]qr \qquad \text{(A14)}$$

wherein $a \equiv \alpha/N$, $k \equiv \kappa_w/N$, and $w_0 \equiv a(L - t_0)/(a + k)$ is the value of the writhe at which the exponent takes its minimum value. We note that $Z(L - w,w)$ is simply the (unnormalized) distribution function for the writhe. It is clear from eq A14 that the effective force constant for fluctuations in net writhe, or equivalently net twist, of a closed circular DNA is $(a + k) = (\alpha + \kappa_w)/N$. Fluctuations in net twist t require simultaneous fluctuations in net writhe w and relax very slowly because (1) the force constant is small and (2) translational motions of long segments of the DNA are required to change the net writhe. Fluctuations in the net twist then do not contribute significantly to the relaxation of the FPA, which probes motions only at times shorter than 150 ns. Instead, the FPA probes primarily those rapid fluctuations in twist of the individual disks that sum nearly to zero and therefore do not produce a significant change in *net* twist of the entire filament. The torsion potential governing those motions is α.

The partition function for a particular topoisomer of a closed circular DNA with constraint L is obtained by integrating eq A13 over w, hence

$$Z_L = \int dw\, Z_L(L - w,w) = \exp[-(ak/(a + k))(L - t_0)^2/2k_BT](2\pi k_BT/(a + k))^{1/2}qr \qquad \text{(A15)}$$

The corresponding free energy is

$$A(L) = -k_BT \ln Z_L = (ak/2(a + k))(L - t_0)^2 - k_BT \ln [(2\pi k_BT/(a + k))^{1/2}qr] \qquad \text{(A16)}$$

The effective force constant for supercoiling is $ak/(a + k)$, which is proportional to N^{-1}. It is customary to express the free energy in terms of the linking-number difference

$$\Delta l = (L - t_0)/2\pi \qquad \text{(A17)}$$

that is, the difference in the number of turns between the unrelaxed and relaxed states. Thus, for a topoisomer with linking number l, the free energy is written

$$A(l) = (g/2)(\Delta l)^2 - k_BT \ln y_L \qquad \text{(A18)}$$

where $y_L \equiv (2\pi k_BT/(a + k))^{1/2}qr$ and $g \equiv (2\pi)^2ak/(a + k)$ is the appropriate force constant. The ratio of equilibrium constants to form topoisomers with two different linking numbers is

$$K(l)/K(m) = \exp[-(A(l) - A(m))/k_BT] = \exp[-(g/2k_BT)((\Delta l)^2 - (\Delta m)^2)] \qquad \text{(A19)}$$

The twist energy parameter E_T is defined as N times the free energy to change Δl from 0 to 1 in units of k_BT, hence

$$E_T \equiv Ng/2k_BT = (2\pi)^2\alpha\kappa_w/(\alpha + \kappa_w)2k_BT \qquad \text{(A20)}$$

Equations A18–A20 agree with the experimental data in regard to the quadratic dependence on $(\Delta l)^2$ and to the variation of the effective force constant g as N^{-1}, or equivalently the constance of E_T at sufficiently large N. Although κ_w should be proportional to κ_β, an analytic expression for the proportionality constant is not available. In spite of this incompleteness, these results are instructive, because they show how the effective force constant for supercoiling, $ak/(a + k)$, differs from that for fluctuations in *net* writhe, or twist, $(a + k)$, and how both are related to the elementary torsion constant α manifested in FPA experiments and in a qualitative way how they are related to the elementary bending constant κ_β. It is also apparent that, given the exact results in eq A10, the assumed Gaussian form in eq A12 is required to obtain agreement with the experimental data in the form of eq A19.

The main result of this section is eq A16, which serves as the starting point for treating the binding of those intercalating dyes whose effect is simply to alter the equilibrium *net* twist t_0 of the unstrained molecule, but not the torque constants α and κ_β. Finally, we caution that eq A14–A20 may apply only to topoisomers belonging to the same family of tertiary conformations.

Supercoiling Free Energy of Intercalated Dye/DNA Complexes. We consider the effect of an intercalated dye on the free energy of supercoiling. We assume that the bound dye does not affect the local torsion and bending constants but acts only to unwind and extend the DNA. The lengthening effect is small compared to the effect of unwinding the DNA, and we neglect it. It is also assumed that dye binding induces no

change in type of secondary structure, except for local unwinding, so the change in equilibrium twist (from t_0) is simply proportional to the amount of bound dye, and there is no need to consider contributions from transitions between secondary structures. Dye binding is assumed to induce no transitions in type of tertiary structure (e.g., from interwound to toroidal), so the effective force constant for writhe, κ_w, remains unaltered. The primary effect of n bound intercalated dyes, then, is to alter the net twist *of the relaxed molecule* from t_0 to

$$t(n) = t_0 - n\phi \tag{A21}$$

where ϕ is the *unwinding* angle. An underwound supercoiled DNA (with $t_0 > L$) is completely relaxed at a particular n^* such that $t(n^*) = L$. Equation A21 then gives $L - t_0 = -n^*\phi$. Replacing t_0 by $t(n)$ in eq A16 yields the supercoiling free energy of dye/DNA complex, which can be written in the form

$$A(L,n) = (g/2)(\phi/2\pi)^2(n - n^*)^2 - k_BT \ln y_L \tag{A22}$$

Dye binding affects y_L only by changing the effective value of N, which is insignificant.

When two different dyes a and b bind to DNA, then

$$t(n_a,n_b) = t_0 - n_a\phi_a - n_b\phi_b \tag{A23}$$

Complete relaxation of an underwound supercoiled DNA in the presence of either dye *alone* occurs at an n_a^* or n_b^* such that $t(n^*) = L$, whence $L - t_0 = -n_a^*\phi_a = -n_b^*\phi_b$. Replacing t_0 by $t(n_a,n_b)$ in eq A16 yields the supercoiling free energy of the two dye/DNA complex, which can be written in the form

$$A(L,n_a,n_b) = [g/2(2\pi)^2][\phi_a^2(n_a - n_a^*)^2 + \phi_b^2(n_b - n_b^*)^2 + \phi_a\phi_b(2n_an_b - n_a^*n_b^*)] - k_BT \ln y_L \tag{A24}$$

Equations A22 and A24 are employed to derive binding isotherms in Appendix B.

Appendix B: Binding of Ligands That Unwind Circular DNA

General Theory. We present a new method for calculating binding isotherms for intercalating ligands that unwind supercoiled DNA but do not alter the twisting and bending force constants. It can readily be generalized to treat simultaneous equilibria involving more than one topoisomer or more than two ligands, and to accommodate cooperative interactions as well as site exclusion. In addition to the assumptions presented in Appendix A, it is also assumed that the intrinsic binding constant, or intrinsic affinity of the dye for an available site, and the unwinding angle are constants, independent of the total amount of bound dye.

The DNA is regarded as a circular lattice containing N sites. Consider the reaction of a closed circular DNA with n_a ligands of type a and n_b ligands of type b to form a specific complex $C_J(n_a,n_b)$ in which the dye molecules are *fixed* at particular lattice sites

$$D + n_a a + n_b b \rightleftharpoons C_J(n_a,n_b) \tag{B1}$$

Each component i is assumed to be dilute and ideal so that it obeys Henry's law

$$\mu_i = \mu_i^0 + k_BT \ln c_i \tag{B2}$$

where c_i is the molarity of the ith species. At equilibrium

$$\mu_D + n_a\mu_a + n_b\mu_b = \mu_{C_J(n_a,n_b)} \tag{B3}$$

We assume that

$$\mu_{C_J(n_a,n_b)}{}^0 - \mu_D{}^0 - n_a\mu_a{}^0 - n_b\mu_b{}^0 = A(L,n_a,n_b) - A(L,0,0) + n_a\bar{F}_a + n_b\bar{F}_b + p_JF_{aa} + q_JF_{bb} + r_JF_{ab} \tag{B4}$$

where $A(L,n_a,n_b)$ is the supercoiling free energy with n_a ligands of type a and n_b ligands of type b bound, as described in Appendix A. $\bar{F}_a$ is the standard free energy change for binding a ligand of type a, and $\bar{F}_b$ applies for binding a b ligand. F_{aa}, F_{bb}, and F_{ab} are the free energies of cooperative interactions, and p_J, q_J, and r_J are the numbers of aa, bb, and ab(ba) junctions or contacts in the Jth configuration. Using eq B2 and B4 in eq B3 yields

$$\frac{c_{C_J(n_a,n_b)}}{c_D} = (c_aK_a)^{n_a}(c_bK_b)^{n_b} \exp[-\Delta A/k_BT] \exp[-(p_JF_{aa} + q_JF_{bb} + r_JF_{ab})/k_BT] \tag{B5}$$

wherein $\Delta A \equiv A(L,n_a,n_b) - A(L,0,0)$, $K_a = \exp[-\bar{F}_a/k_BT]$, and $K_b = \exp[-\bar{F}_b/k_BT]$. The total concentration of all complexes with n_a,n_b bound ligands is

$$c_{C(n_a,n_b)} = \sum_J c_{C_J(n_a,n_b)} = c_D(c_aK_a)^{n_a}(c_bK_b)^{n_b} \exp[-\Delta A/k_BT]W(n_a,n_b) \tag{B6}$$

where

$$W(n_a,n_b) \equiv \sum_J \exp[-(p_JF_{aa} + q_JF_{bb} + r_JF_{ab})/k_BT] \tag{B7}$$

In the absence of cooperative interactions of any ligand, $F_{aa} = 0 = F_{bb} = F_{ab}$, and $W(n_a,n_b)$ is just the number of distinct configurations with n_a,n_b bound ligands. However, we do not yet invoke the simplifying assumption. The total concentration of all complexes is

$$c_C = \sum_{n_a}\sum_{n_b} c_{C(n_a,n_b)} = c_D\sum_{n_a}\sum_{n_b}(c_aK_a)^{n_a}(c_bK_b)^{n_b} \exp[-\Delta A/k_BT]W(n_a,n_b) = c_DG \tag{B8}$$

where

$$G = \sum_{n_a}\sum_{n_b}(c_aK_a)^{n_a}(c_bK_b)^{n_b} \exp[-\Delta A/k_BT]W(n_a,n_b) \tag{B9}$$

is a kind of grand partition function. The average number of a ligands bound *per complex* is

$$\bar{n}_a = \sum_{n_a}\sum_{n_b} n_a c_{C(n_a,n_b)} / \sum_{n_a'}\sum_{n_b'} c_{C(n_a',n_b')} = c_a\partial \ln G/\partial c_a \tag{B10}$$

Similarly, the average number of b ligands bound *per complex* is

$$\bar{n}_b = c_b\partial \ln G/\partial c_b \tag{B11}$$

We have also a concentration for the total number of DNA molecules

$$c_D{}^0 = c_D + c_C \tag{B12}$$

Use of eq B8 leads to

$$c_C = c_D{}^0\frac{G}{1 + G} \tag{B13}$$

When many dye molecules are bound per complex, but not totally cooperatively, $G \gg 1$ and $c_C \cong c_D{}^0$. In that case, the overall binding ratios become

$$r_a \equiv \frac{\bar{n}_ac_C}{Nc_D{}^0} \cong \frac{\bar{n}_a}{N} = \frac{c_a}{N}\frac{\partial \ln G}{\partial c_a} \tag{B14}$$

$$r_b \equiv \frac{\bar{n}_bc_C}{Nc_D{}^0} \cong \frac{\bar{n}_b}{N} = \frac{c_b}{N}\frac{\partial \ln G}{\partial c_b} \tag{B15}$$

In other words, the overall binding ratios are just those of the

complexes when most of the DNA is complexed. Although eq B14 and B15 are usually evaluated directly for linear DNAs, we must take an alternative route for supercoiled DNAs.

When many dye molecules are bound, G is very large, and we can approximate ln G by the logarithm of its maximum term (Hill, 1960). To do this, we must determine the $\bar{n}_a,\bar{n}_b$ for which ln (term) is maximal. These values must satisfy

$$\frac{\partial}{\partial n_a}[n_a \ln (c_aK_a) + n_b \ln (c_bK_b) - \Delta A/k_BT + \ln W(n_a,n_b)] = 0 \quad \text{(B16)}$$

$$\frac{\partial}{\partial n_b}[n_a \ln (c_aK_a) + n_b \ln (c_bK_b) - \Delta A/k_BT + \ln W(n_a,n_b)] = 0 \quad \text{(B17)}$$

From eq A24 we obtain

$$\frac{\partial}{\partial n_a}[A(L,n_a,n_b) - A(L,0,0)] = g/(2\pi)^2(\phi_a{}^2(n_a - n_a{}^*) + \phi_a\phi_b n_b) \quad \text{(B18)}$$

$$\frac{\partial}{\partial n_b}[A(L,n_a,n_b) - A(L,0,0)] = g/(2\pi)^2(\phi_b{}^2(n_b - n_b{}^*) + \phi_a\phi_b n_a) \quad \text{(B19)}$$

After taking the derivative in eq B16 with the help of eq B18, we can solve for c_a^{-1} and multiply by r_a to obtain

$$r_a/c_a = K_a \exp[(g/k_BT)((\phi_a/2\pi)^2(n_a{}^* - n_a) - (\phi_a\phi_b/(2\pi)^2)n_b)]X_a(n_a,n_b) \quad \text{(B20)}$$

where

$$X_a(n_a,n_b) \equiv r_a \exp[\partial \ln W/\partial n_a]_{\bar{n}_a,\bar{n}_b} \quad \text{(B21)}$$

and the derivative is evaluated at $\bar{n}_a = r_aN$ and $\bar{n}_b = r_bN$. Similarly, we obtain

$$r_b/c_b = K_b \exp[(g/k_BT)((\phi_b/2\pi)^2(n_b{}^* - n_b) - (\phi_a\phi_b/(2\pi)^2)n_a)]X_b(n_a,n_b) \quad \text{(B22)}$$

where

$$X_b(n_a,n_b) \equiv r_b \exp[\partial \ln W/\partial n_b]_{\bar{n}_a,\bar{n}_b}$$

These binding isotherms are obtained in terms of the unknown $X_a(n_a,n_b)$ and $X_a(n_a,n_b)$ by applying the conditions for the maximum term without explicitly evaluating that term. Of course, to evaluate $X_a(n_a,n_b)$ and $X_b(n_a,n_b)$, it is necessary to evaluate $W(n_a,n_b)$ by some means. The important point is that in the absence of supercoiling, or if $g = 0$, so the supercoiling free energy is 0, we obtain simply

$$r_a/c_a = K_aX_a(n_a,n_b) \quad \text{(B23)}$$

$$r_b/c_b = K_bX_b(n_a,n_b) \quad \text{(B24)}$$

$X_a(n_a,n_b)$ and $X_b(n_a,n_b)$ are derived from $W(n_a,n_b)$, which is given in eq B7. If the cooperative interaction parameters F_{aa}, F_{bb}, and F_{ab} remain the same in the presence and absence of supercoiling, as assumed here, then so will W, X_a, and S_b! Thus, if the binding isotherms for r_a/c_a and r_b/c_b have been derived, or measured, for the DNA *in the absence of supercoiling* by any means, then $X_a(n_a,n_b)$ can be immediately determined by comparison with eq B23 and $X_b(n_a,n_b)$ determined by comparison with eq B24. For example, the theoretical results of McGhee and von Hippel (1974) for r_a/c_a suffice to determine $X_a(n_a,n_b)$ and $X_b(n_a,n_b)$ for a variety of special cases.

The present treatment differs from that of Hsieh and Wang (1975) and Bauer and Vinograd (1970) in that the simultaneous binding of two different ligands is considered, and absolute, as well as relative, binding isotherms are predicted. In addition, the conditions for validity of their treatments, namely that $G \gg 1.0$ (essentially no uncomplexed DNA) and ln G = ln (maximum term) are made apparent. Finally, the present theory allows the treatment of fluctuations and can be generalized to allow the treatment of circumstances outside the domain of validity of those earlier works (e.g., $G \ll 1.0$).

Noncooperative Neighbor-Exclusion Model. For nonsupercoiled DNAs, the isotherms r_a/c_a and r_b/c_b for the simultaneous binding of two dyes, both of which exclude two sites upon binding but otherwise do not interact, are presented by McGhee and von Hippel (1974) and can also be obtained by using the matrix method (J. M. Schurr, unpublished calculation). For example

$$r_a/c_a = K_a\frac{(1 - 2(r_a + r_b))^2}{(1 - (r_a + r_b))} \quad \text{(B25)}$$

and the corresponding equation holds for r_b/c_b. Comparison with eq B23 and B24 gives $X_a(r_a,r_b) = (1 - 2(r_a + r_b))^2/(1 - (r_a + r_b))$, and in this case $X_b(r_a,r_b)$ is the same. Thus, eq B20 and B22 for supercoiled DNAs become

$$r_a/c_a = K_a \exp[(gN/k_BT)((\phi_a/2\pi)^2(r_a{}^* - r_a) - (\phi_a\phi_b/(2\pi)^2)r_b)]\frac{(1 - 2(r_a + r_b))^2}{(1 - (r_a + r_b))} \quad \text{(B26)}$$

$$r_b/c_b = K_b \exp[(gN/k_BT)((\phi_b/2\pi)^2(r_b{}^* - r_b) - (\phi_a\phi_b/(2\pi)^2)r_a)]\frac{(1 - 2(r_a + r_b))^2}{(1 - (r_a + r_b))} \quad \text{(B27)}$$

If we further specialize to the case when one species, say a, is present only in minute amounts so that (1) $r_a \ll r_b$, (2) $r_a\phi_a \ll r_b\phi_b$, (3) $r_a \ll r_a{}^*$, and (4) $r_a \ll r_b{}^*$, then these expressions reduce to

$$r_a/c_a = K_a \exp[a_{ab}(r_b{}^* - r_b)](1 - 2r_b)^2/(1 - r_b) \quad \text{(B28)}$$

$$r_b/c_b = K_b \exp[a_b(r_b{}^* - r_b)](1 - 2r_b)^2/(1 - r_b) \quad \text{(B29)}$$

where

$$a_{ab} = (gN/k_BT)(\phi_a/2\pi)(\phi_b/2\pi) \quad \text{(B30)}$$

and

$$a_b = (gN/k_BT)(\phi_b/2\pi)^2 \quad \text{(B31)}$$

Equations B28 and B29 are recognized as eq 7 and 4, respectively, in the text, when species a is ethidium and b is chloroquine. Equation B29 is also the isotherm for binding of b in the absence of a.

Registry No. Chloroquine, 54-05-7; ethidium, 3546-21-2.

References

Allison, S. A., & Schurr, J. M. (1979) *Chem. Phys. 41*, 35–59.

Allison, S. A., Shibata, J. H., Wilcoxon, L., & Schurr, J. M. (1982) *Biopolymers 21*, 729–762.

Ashikawa, I., Kinosita, K., Jr., Ikegami, A., Nishimura, Y., Tsuboi, M., Watanabe, K., & Iso, K. (1983) *J. Biochem. (Tokyo) 93*, 665–668.

Ashikawa, I., Kinosita, K., Jr., & Ikegami, A. (1984) *Biochim. Biophys. Acta 782*, 87–93.

Assa-Munt, N., Granot, J., Behling, R. W., & Kearns, D. R. (1984) *Biochemistry 23*, 944–955.

Barkley, M. D., & Zimm, B. H. (1979) *J. Chem. Phys. 70*, 2991–3007.

Bauer, W. (1978) *Annu. Rev. Biophys. Bioeng. 7*, 287–313.

Bauer, W., & Vinograd, J. (1970) *J. Mol. Biol. 47*, 419–435.

Benight, A. S., Schurr, J. M., Flynn, P. F., Reid, B. R., & Wemmer, D. E. (1988) *J. Mol. Biol. 200*, 377–399.
Bresloff, J. L., & Crothers, D. M. (1981) *Biochemistry 20*, 3547–3553.
Chandrasekaran, S., Jones, R. L., & Wilson, W. D. (1985) *Biopolymers 24*, 1963–1979.
Cohen, S. N., & Yielding, K. L. (1965) *J. Biol. Chem. 240*, 3123–3131.
Crick, F. H., & Klug, A. (1975) *Nature (London) 255*, 530–533.
Dahl, K. S., Pardi, A., & Tinoco, I., Jr. (1982) *Biochemistry 21*, 2730–2737.
Delben, F., Quadrifoglio, F., Giancotti, V., & Crescenzi, V. (1982) *Biopolymers 21*, 331–341.
Depew, R. E., & Wang, J. C. (1975) *Proc. Natl. Acad. Sci. U.S.A. 72*, 4275–4279.
Englander, S. W., & Kallenbach, N. R. (1983) *Q. Rev. Biophys. 16*, 521–655.
Englander, S. W., Kallenbach, N. R., Heeger, A. J., Krumhansl, J. D., & Litwin, S. (1980) *Proc. Natl. Acad. Sci. U.S.A. 77*, 7222–7226.
Fox, K. R., & Waring, M. J. (1984) *Nucleic Acids Res. 12*, 9271–9285.
Fujimoto, B. S., Shibata, J. H., Schurr, R. L., & Schurr, J. M. (1985) *Biopolymers 24*, 1009–1022.
Fujimoto, B. S., Wu, P. G., Song, L., Clendenning, J. B., & Schurr, J. M. (1988) *Biophys. J. 53*, 307a.
Fuller, F. B. (1971) *Proc. Natl. Acad. Sci. U.S.A. 68*, 815–819.
Genest, D., Mirau, P. A., & Kearns, D. R. (1985) *Nucleic Acids Res. 13*, 2603–2615.
Graves, D. E., & Krugh, T. R. (1983) *Anal. Biochem. 134*, 73–81.
Hertzberg, R. P., & Dervan, P. B. (1984) *Biochemistry 23*, 3934–3945.
Hill, T. L. (1960) *An Introduction to Statistical Thermodynamics*, pp 478–480, Addison-Wesley, Reading, MA.
Hinton, D. M., & Bode, V. C. (1975) *J. Biol. Chem. 250*, 1061–1079.
Hogan, M. E., & Jardetzky, O. (1979) *Proc. Natl. Acad. Sci. U.S.A. 76*, 6341–6345.
Hogan, M. E., & Jardetzky, O. (1980) *Biochemistry 19*, 2079–2085.
Horowitz, D., & Wang, J. C. (1984) *J. Mol. Biol. 173*, 75–91.
Hsieh, T. S., & Wang, J. C. (1975) *Biochemistry 14*, 527–535.
Jones, M. B., Hollstein, U., & Allen, F. S. (1987) *Biopolymers 26*, 121–135.
Jones, R. L., Lanier, A. C., Keel, R. A., & Wilson, W. D. (1980) *Nucleic Acids Res. 8*, 1613–1624.
Kastrup, R. V., Young, M. A., & Krugh, T. R. (1978) *Biochemistry 17*, 4855–4865.
Krugh, T. R., & Reinhardt, C. G. (1975) *J. Mol. Biol. 97*, 133–162.
Krugh, T. R., Wittling, F. N., & Cramer, S. R. (1975) *Biopolymers 14*, 197–210.
Lamos, M. L., Lobenstine, E. W., & Turner, D. H. (1986) *J. Am. Chem. Soc. 108*, 4278–4284.
Langowski, J., Fujimoto, B. S., Wemmer, D. E., Benight, A. S., Drobny, G., Shibata, J. H., & Schurr, J. M. (1985a) *Biopolymers 24*, 1023–1056.
Langowski, J., Benight, A. S., Fujimoto, B. S., Schurr, J. M., & Schomburg, U. (1985b) *Biochemistry 24*, 4022–4028.
Le Bret, M. (1979) *Biopolymers 18*, 1709–1725.
Le Bret, M. (1980) *Biopolymers 19*, 619–637.
Le Bret, M. (1984) *Biopolymers 23*, 1835–1867.
Le Pecq, J. B., & Paoletti, C. (1967) *J. Mol. Biol. 27*, 87–106.
Levene, S. D., & Crothers, D. M. (1986) *J. Mol. Biol. 189*, 73–83.
Lin, S. C., Thomas, J. C., Allison, S. A., & Schurr, J. M. (1981) *Biopolymers 20*, 209–230.
Low, C. M. L., Drew, H. R., & Waring, M. J. (1984) *Nucleic Acids Res. 12*, 4865–4879.
Macgregor, R. B., Jr., Clegg, R. M., & Jovin, T. M. (1985) *Biochemistry 24*, 5503–5510.
Magde, D., Zappola, M., Knox, W. H., & Nordland, T. M. (1983) *J. Phys. Chem. 87*, 3286–3288.
Mandal, C., Kallenbach, N. R., & Englander, S. W. (1979) *J. Mol. Biol. 135*, 391–411.
McGhee, J. D., & von Hippel, P. H. (1974) *J. Mol. Biol. 86*, 469–489.
Millar, D. P., Robbins, R. J., & Zewail, A. H. (1982) *J. Chem. Phys. 76*, 2080–2094.
Mirau, P. A., Behling, R. W., & Kearns, D. R. (1985) *Biochemistry 24*, 6200–6211.
Müller, W., & Crothers, D. M. (1975) *Eur. J. Biochem. 54*, 267–277.
Nelson, J. W., & Tinoco, I., Jr. (1984) *Biopolymers 23*, 213–233.
Patel, D. J., & Canuel, L. L. (1976) *Proc. Natl. Acad. Sci. U.S.A. 73*, 3343–3347.
Patel, D. J., & Canuel, L. L. (1979) *Eur. J. Biochem. 96*, 267–276.
Preisler, R. S., Mandal, C., Englander, S. W., Kallenbach, N. R., Frazier, J., Miles, H. T., & Howard, F. B. (1984) *Biopolymers 23*, 2099–2125.
Pulleyblank, D. E., Shure, M., Tang, D., Vinigrad, J., & Vosberg, H. P. (1975) *Proc. Natl. Acad. Sci. U.S.A. 72*, 4280–4284.
Reinhardt, C. G., & Krugh, T. R. (1978) *Biochemistry 17*, 4845–4854.
Scamrov, A. V., & Beabealashvilli, R. Sh. (1983) *FEBS Lett. 164*, 97–101.
Schurr, J. M. (1984) *Chem. Phys. 84*, 71–96.
Schurr, J. M., & Fujimoto, B. S. (1988) *Biopolymers* (in press).
Shibata, J. H., Wilcoxon, J., Schurr, J. M., & Knauf, V. (1984) *Biochemistry 23*, 1188–1194.
Shibata, J. H., Fujimoto, B. S., & Schurr, J. M. (1985) *Biopolymers 24*, 1909–1930.
Shore, D., & Baldwin, R. L. (1983) *J. Mol. Biol. 170*, 957–1007.
Skinner, J. L. (1983) *J. Chem. Phys. 79*, 1955–1964.
Skinner, J. L., & Wolynes, P. G. (1980a) *J. Chem. Phys. 73*, 4015–4021.
Skinner, J. L., & Wolynes, P. G. (1980b) *J. Chem. Phys. 73*, 4022–4025.
Sobell, H. M., Tsai, C. C., Jain, S. C., & Gilbert, S. G. (1977) *J. Mol. Biol. 114*, 333–365.
Sobell, H. M., Sakove, T. D., Banerjee, J. A., Bhandary, K. K., Reddy, B. S., & Lozansky, E. D. (1983) *Cold Spring Harbor Symp. Quant. Biol. 47*, 293–314.
Song, L., Fujimoto, B. S., & Schurr, J. M. (1988) *Biophys. J. 53*, 306a.
Stoller, D., & Levine, L. (1963) *Arch. Biochem. Biophys. 101*, 335–341.
Teitelbaum, H., & Englander, S. W. (1975a) *J. Mol. Biol. 92*, 55–78.
Teitelbaum, H., & Englander, S. W. (1975b) *J. Mol. Biol. 92*, 79–92.
Thomas, J. C., & Schurr, J. M. (1983) *Biochemistry 22*, 6194–6198.

Thomas, J. C., Allison, S. A., Appellof, C. J., & Schurr, J. M. (1980a) *Biophys. Chem. 12*, 177–188.
Thomas, J. C., Allison, S. A., Schurr, J. M., & Holder, R. D. (1980b) *Biopolymers 19*, 1451–1474.
Van Dyke, M. W., & Dervan, P. B. (1984) *Science (Washington, D.C.) 225*, 1122–1127.
Van Dyke, M. W., Hertzberg, R. P., & Dervan, P. B. (1982) *Proc. Natl. Acad. Sci. U.S.A. 79*, 5470–5474.
Volodoskii, A. V., Anshelevich, V. V., Lukashin, A. V., & Frank-Kamenetskii, M. D. (1979) *Nature (London) 280*, 294–298.
Wang, J. C. (1974) *J. Mol. Biol. 89*, 783–801.
Waring, M. J. (1965) *J. Mol. Biol. 13*, 269–282.
Wilcoxon, J., & Schurr, J. M. (1983) *Biopolymers 22*, 2273–2321.
Wilcoxon, J., Shibata, J. H., Thomas, J. C., & Schurr, J. M. (1982) in *Biomedical Applications of Laser Light Scattering* (by Lee, W. I., Sattelle, D., & Ware, B.) pp 27–36, Elsevier Biomedical, Amsterdam.
Wilcoxon, J., Schurr, J. M., & Warren, R. A. J. (1984) *Biopolymers 23*, 767–774.
Wilson, W. D., Krishnamoorthy, C. R., Wang, Y. H., & Smith, J. C. (1985) *Biopolymers 24*, 1941–1961.
Winkle, S. A., Rosenberg, L. S., & Krugh, T. R. (1982) *Nucleic Acids Res. 10*, 8211–8223.
Wu, P. G., Fujimoto, B. S., & Schurr, J. M. (1987) *Biopolymers 26*, 1463–1488.
Wu, P. G., Benight, A. S., & Schurr, J. M. (1988) *Biophys. J. 53*, 307a.

Anthracycline–DNA Interactions Studied with Linear Dichroism and Fluorescence Spectroscopy†

Magdalena Eriksson, Bengt Nordén,* and Svante Eriksson
Department of Physical Chemistry, Chalmers University of Technology, and University of Göteborg, S-412 96 Göteborg, Sweden

Received April 4, 1988; Revised Manuscript Received June 20, 1988

ABSTRACT: DNA-binding geometry and dynamics of a number of anthracyclines, including adriamycin and 4-demethoxydaunorubicin, interacting with DNA have been studied by means of linear dichroism and fluorescence techniques. The anthracycline chromophore is found to be approximately parallel to the plane of the DNA bases and to have a restricted mobility, as would be expected for an intercalative binding mode, but there are variations between different directions in the chromophore as well as between the drugs. From dichroic spectra of adriamycin in an anisotropic host of poly(vinyl alcohol), absorption components corresponding to transitions with mutually orthogonal polarizations have been resolved. These can be exploited to determine the orientations of the two chromophore axes in the DNA complex relative to the DNA helix axis. In a certain binding regime the long axis of the bound anthracycline chromophores (with the exception of 4-demethoxydaunorubicin) is found to be approximately 10° closer to perpendicular to the helix axis than are the DNA bases. This demonstrates that the average base tilt is at least 10°. By contrast, the short axis of the aglycon moiety is found to be tilted some 20–30° from perpendicular. This may be because it is probing a base direction with a more pronounced, static or dynamic, inclination than the average in DNA. The drug orientation and the DNA orientation (reflecting flexibility) are observed to vary differently and nonmonotonically with binding ratio, suggesting specific binding and varying site geometries. The fluorescence lifetimes of adriamycin and 4-demethoxydaunorubicin in aqueous solution are measured to 1.0 and 1.5 ns, respectively, and are found to change only moderately upon binding to poly(dA-dT) or poly(dG-dC). A high fluorescence polarization anisotropy shows that the anthracyclines in their DNA complexes have a restricted mobility on the time scale of their fluorescence lifetimes. Comparison with ethidium, though, indicates a significantly higher degree of libration of the anthracyclines. This effect is discussed in terms of a selective fluorescence detection of drug molecules that, owing to DNA breathing or (slow) exchange, are in a transient state of semiintercalation.

The anthracycline antibiotics include several hundreds of compounds, isolated from nature or synthesized by man. Many of them are biologically active and are used in cancer chemotherapy; among the various drugs exhibiting efficiencies toward different kinds of solid tumors and leukemia, adriamycin (AM) and daunorubicin (DR) (Figure 1) are the most well-known (Arcamone, 1981).

Nuclear DNA is believed to be the primary target of antitumor activity of the anthracyclines, resulting in inhibition of DNA transcription and replication. In vitro, the anthracycline–DNA interaction mainly occurs by intercalation of the planar ring system between DNA base pairs. The DNA interaction in vivo has been documented by numerous biochemical studies and from structure–activity relationships: compounds that have reached the clinical stage, for example, generally belong to the group with the highest affinity for DNA (Arcamone & Penco, 1987). The planar aromatic aglycon group, which can intercalate, together with the positively charged amino–sugar moiety can be anticipated to provide a high DNA affinity as has been evidenced from binding studies (Valentini, private communication). [It may be noted, though,

† This project was supported by the Swedish Natural Science Research Council.

0006-2960/88/0427-8144$01.50/0